

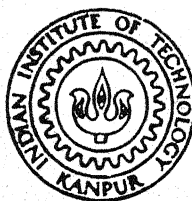
A STUDY IN APPLICATION OF METHOD OF SUCCESSIVE ITERATION TO THE ANALYSIS OF LAMINATED COMPOSITE PLATES

by

G. RADHAKRISHNAN

TH
AE/1989/m
R1185

AE
1989
M
RAD
STU



DEPARTMENT OF AERONAUTICAL ENGINEERING
INDIAN INSTITUTE OF TECHNOLOGY KANPU

JUNE 1989

A STUDY IN APPLICATION OF METHOD OF SUCCESSIVE ITERATION TO THE ANALYSIS OF LAMINATED COMPOSITE PLATES

A Thesis Submitted
in Partial Fulfilment of the Requirements
for the Degree of

MASTER OF TECHNOLOGY

by

G. RADHAKRISHNAN

to the

**DEPARTMENT OF AERONAUTICAL ENGINEERING
INDIAN INSTITUTE OF TECHNOLOGY KANPUR**

JUNE 1989

AE-1989-M-RAD-APP

- 4 APR 1990


CENTRAL LIBRARY
I. I. T., KANPUR

Acc. No. **A107256**

CERTIFICATE

This is to certify the work "A STUDY IN APPLICATION OF METHOD OF SUCCESSIVE ITERATION TO THE ANALYSIS OF LAMINATED COMPOSITE PLATES", by G. Radha Krishnan has been carried out under my supervision and has not been submitted elsewhere for a degree.

30 June, 1989.



(V.K. GUPTA)
Assistant Professor
Department of Aeronautical Engineering
Indian Institute of Technology
Kanpur

ACKNOWLEDGEMENTS

I wish to express my gratitude to my thesis supervisor Dr. V.K. Gupta for his invaluable guidance, critical supervision and constant encouragement throughout this work. I wish to thank Dr. N.G.R. Iyengar for his valuable suggestions during my M.Tech. study.

I sincerely thank Ramesh A.S., Longwal, Gundu, Bacha, Sampath, Kanaku, Rasu, Pandimani, Seshadri, Raghunandan, Kavirayar, Shah Nawas, Suri Pandi, Victor, Ilavarasar, Anbu. M.D.R., Sen, Rajasankar and all the members of mangai mandram.

Thanks are also due to Mr. U.S. Misra for his excellent typing in short duration.

(G. RADHAKRISHNAN)

TABLE OF CONTENTS

ABSTRACT
LIST OF TABLES
LIST OF FIGURES
SYMBOLS AND NOTATION

CHAPTER 1 INTRODUCTION AND LITERATURE SURVEY

- 1.1 Introduction
- 1.2 Literature Survey
- 1.3 Limitations of Earlier Methods
- 1.4 Scope of the Present Work

CHAPTER 2 GENERAL ANALYSIS OF COMPOSITE PLATES

- 2.1 Assumptions in Thin Composite Plate Theory
- 2.2 Analysis
- 2.3 Governing Equations of Antisymmetric Angle Ply Laminates
- 2.4 Boundary Conditions of Antisymmetric Angle Ply Laminates
- 2.5 Levy's Solution Procedure
- 2.6 Development of the Solution Technique
- 2.7 Expression for the Eigen value
- 2.8 Expression for the Decoupling Thickness Ratios

CHAPTER 3 ANALYSIS OF DECOUPLED LAMINATES

- 3.1 Biaxial Buckling Problems
- 3.2 Free Vibration Problems
- 3.3 Numerical Computations
- 3.4 Results and Discussions
- 3.5 General Observations

CHAPTER 4 ANALYSIS OF COUPLED LAMINATES

- 4.1 Governing Equations
- 4.2 Rayleigh's Quotient
- 4.3 Boundary Condition
- 4.4 General Steps in Successive Technique
- 4.5 Iteration Sequences in Models
- 4.6 Numerical Study in Models
- 4.7 Detailed Numerical Analysis in Model
- 4.8 Solution Using Two Variables v and w
- 4.9 Numerical Study with Two Variables
- 4.10 General Observations

CHAPTER 5 CONCLUSION

REFERENCES

ABSTRACT

The analysis of composite plate is an increasing interest in aerospace structures. Various methods available in the literature have limitations in terms of computational efficiency. It is considered as an important criteria in optimal design. Keeping in view, a study has been made to apply successive iteration method in the analysis of laminated plates.

By Levy's solution procedure, the governing partial differential equations of the plate are converted to ordinary differential equations. The iteration technique is then applied to eigen value plate problems. Both coupled and decoupled antisymmetric laminates have been considered in the present study.

In decoupled laminates, biaxial buckling problems are investigated in cases with x edges simply supported and y edges in simply supported, simply supported-clamped, clamped, clamped-free, simply supported-free and free boundary conditions. Free vibration problems are also investigated in cases with x edges simply supported and y edges simply supported, clamped, and free boundary conditions. Computations were carried out on Glass-epoxy and carbon-epoxy homogeneous laminates for different as

ratios, fibre orientations and buckling load ratios. The eigen values, buckling load or natural frequency obtained using this technique agrees closely with the earlier methods. The technique consumes less, computational time and requires less efforts. The technique is independent of initial starting functions. Optimal design of thin laminates can be made readily, applying this technique with decoupled condition.

In coupled laminates uniaxial buckling problem is investigated in case with x edges simply supported and y edges clamped condition. Various computational model schemes with three and two dependent coupling variables failed to give correct result, even though convergence in eigen value was achieved. This may be due to sensitiveness of the coefficients of the derivatives appearing in the governing equations of laminate.

LIST OF FIGURES

Fig.No.	Caption	Page
2.1	Geometry of n-layered laminate.	28
2.2	Unidirectionally reinforced laminae.	29
2.3	Positive rotation of lamina axes by θ w.r.t. laminate axes.	30
2.4	Loading and geometry of rectangular plate.	31
2.5	Geometry of a six-layered laminate.	32
3.1	Variation of nondimensional buckling load (λ) with fibre orientation (θ) . ($K = 0.0$, $AR = 1.0$)	47
3.2	Variation of nondimensional buckling load (λ) with fibre orientation (θ) . ($K = 2.0$, $AR = 2.0$) .	47
3.3	Variation of nondimensional buckling load (λ) with aspect ratio (AR) . ($K = 0.0$, $\theta = 30^\circ$) .	48
3.4	Variation of nondimensional buckling load (λ) with aspect ratio (AR) . ($K = 1.0$, $\theta = 60^\circ$) .	48
3.5	Variation of nondimensional buckling load (λ) with buckling load ratio (K) . ($AR = 1.0$, $\theta = 30^\circ$) .	49
3.6	Variation of nondimensional buckling load (λ) with buckling load ratio (K) ($AR = 2.0$, $\theta = 60^\circ$) .	49

Fig.No.	Caption	Page
3.7	Variation of nondimensional buckling load (λ) with aspect ratio (AR). ($K = 0.0$, $AR = 1.0$).	50
3.8	Variation of nondimensional frequency ($\sqrt{\lambda_f}$) with aspect ratio (AR). ($\theta = 30^\circ$).	50
3.9	Variation of nondimensional natural frequency ($\sqrt{\lambda_f}$) with fibre orientation (θ). ($AR = 1.0$).	51
3.10	Variation of nondimensional natural frequency ($\sqrt{\lambda_f}$) with fibre orientation (θ). ($AR = 2.0$).	51

LIST OF TABLES

Table No.	Caption	Page
3.1.	Effect of Aspect Ratios in Decoupled Laminate	45
3.2.	Effect of Starting Functions, Mesh Size .. And Convergence Criteria in Decoupled Laminate	46
4.1.	Effect of Fibre Orientations in the Convergence Study ..	76
4.2.	Effect of Starting Functions, Initial Eigen Value and Computations in Double Precision ..	77
4.3.	Convergence Study of Buckling Load in Various Model Schemes ..	78
4.4.	Effect of Number of Layers in Model 5 ..	79
4.5.	Effect of Starting Functions and Length to Thickness Ratio in Model 5 ..	80
4.6.	Convergence Study of Constants of Integration and Displacement Functions in Model 5 ..	81
4.7.	Convergence Study of Particular Integral Terms in Model 5 ..	82
4.8.	Iterated Eigen Value in Solution Using Two Variables V and W ..	83

SYMBOLS AND NOTATIONS

a	-	Length of the plate in x-direction
b	-	Length of the plate in y-direction
h	-	Total thickness of a laminate
$E_1, E_2, E_{12}, \nu_{12}$	-	Elastic constants of fibre material
Q_{ij}	-	Reduced stiffnesses
$\sigma_1, \sigma_2, \sigma_3$	-	Inplane stresses
$\epsilon_1, \epsilon_2, \epsilon_3$	-	Inplane strain components
$\bar{Q}_{ij\theta}$	-	Transformed, reduced stiffnesses
θ_i	-	Fibre orientation in i^{th} lamina
t_i	-	Thickness of i^{th} lamina
ρ	-	Average density of the laminate
$A_{ij}, B_{ij}, D_{ij}, E_{ij}$	-	Elastic constants of a laminate plate
z_i	-	Distance of i^{th} lamina from geometric mid plane of the laminate
R_1	-	t_1/t_3 is the thickness ratio of a six layered laminate
R_2	-	t_2/t_3 is the thickness ratio of a six layered laminate
r	-	Length to thickness ratio = a/h
p	-	Aspect ratio of the plate = a/b
m	-	Mode number
α	-	$m\pi$
u, v	-	Mid-plane linear displacements in x and y directions respectively

w	-	Lateral linear displacement
ψ_x	-	Mid plane rotational displacement of normal about x-axis
ψ_y	-	Mid plane rotational displacement of normal about y-axis
$\epsilon_x, \epsilon_y, \epsilon_{xy}$	-	Mid plane strains in x-y plane
k_x, k_y, k_{xy}	-	Curvatures in the x-y plane
N_x, N_y, N_{xy}	-	Resultant forces acting on a laminate
M_x, M_y, M_{xy}	-	Resultant moments acting on a laminate
\bar{N}_x, \bar{N}_y	-	Applied inplane forces per unit width
K	-	Buckling load ratio = \bar{N}_y / \bar{N}_x
ω	-	Natural frequency of vibration
λ	-	Non-dimensional buckling load factor $\lambda = \frac{\bar{N}_x b^2}{E_2 h^3}$
λ_E	-	Non-dimensional natural frequency = $\frac{\rho a^2 b^2}{E_2 h^3}$
π_0	-	Total potential energy of the laminate.

CHAPTER-I

INTRODUCTION AND LITERATURE SURVEY

1.1 INTRODUCTION

Fibre reinforced composite plates have been widely used in the primary structures of aircrafts and spacecrafts because of their high specific strength and stiffnesses. The anisotropic properties can be tailored to the structural requirements by a judicious selection of lamination stacking sequence, fibre orientations, number of plies and thickness of individual lamina. This flexibility in design leads to overall weight reduction. The other advantages such as durability, ease of repair, high energy absorption and seamless construction offer an attractive alternative to metallic aircraft structural components.

Composites exhibit shear extension and bending-stretching coupling, unlike isotropic materials. Couplings are undesirable as it causes warping of laminates and increases the complexity in analysis. Their presence reduces strength and stiffnesses of laminates considerably. It is possible to eliminate the effect of coupling by suitably manipulating thicknesses, fibre orientations and stacking sequence. For optimal composite plate design decoupled laminates may have to be used. An efficient technique is desirable for optimal design of composite plates, which tend

to decouple at the optimum point [17] . A detailed literature survey has been made in the techniques available for the analysis of composite plates.

1.2 LITERATURE SURVEY

Timoshenko and Krieger [1] studied the buckling of isotropic homogeneous plates.

Harris, G.Z. [2] studied the buckling of uniaxially and biaxially loaded orthotropic plates using Ritz variational technique.

Warren and Norris [3] suggested that for the laminates containing laminae of identical orthotropic properties and thicknesses. It is possible to orient the layers in such a way that the resultant elastic stretching behaviour is isotropic. According to them, to achieve this result, the total number of layers must be three or more and a typical K th layer of a N -layered laminate must be oriented at an angle $\theta_k = (K-1)/n$. However this laminate is not isotropic with regard to bending-stretching coupling.

Barthalme [4] suggested that for uncoupled, orthotropic laminates made of laminae of identical thicknesses and material properties, it is possible to achieve inplane orthotropy as well orthotropy in bending by selection of suitably ply stacking order. The fibres lie symmetrically about the orthotropic axes of the laminate.

Ambartsumyan [5] recognised the effect of coupling between inplane stretching and plate bending. This coupling effect is the major difference between elastic response of an arbitrarily laminated and homogeneous plates.

Holston [6] analysed the buckling response of orthotropic plates with three simply supported and the remaining edge free by developing an approximate equation for the buckling load.

Sharma, Iyengar and Murthy [7] have shown that it is possible to eliminate the coupling effects in four and six layered antisymmetric cross ply laminates by a suitable choice of thickness ratios of laminae. Thickness ratios are shown to be independent of material properties.

Jones [8] analysed the buckling and dynamic response of antisymmetrically laminated angle ply rectangular plates using closed form approach.

Housner and Stein [9] used a finite difference energy analysis method to make parametric studies for angle ply simply supported and clamped graphite - epoxy plates having a large number of alternating plies ($\pm \theta$).

Paul, Jensen, Flinch [10] examined the effects of inherent mechanical couplings exhibited in fully anisotropic (i.e. unsymmetric) graphite/epoxy laminates on the buckling loads and mode shapes. The results indicate that the coupling especially those which relate stretching and bending behaviour

cause out of plane deflections prior to buckling and reduce the buckling load significantly. The analytical results also show that the mode shapes exhibit twisting due to mechanical coupling.

Klaus Rohwer [11] has analysed the plate with different boundary conditions edge ratios and fibre angles under uniaxial as well as biaxial normal stresses to see the bending-twisting coupling on the buckling load of symmetrically stacked plates. An indicator is established which allows to approximately determine the buckling load reduction with the aid of stiffness coefficients alone. For plates under compression it allows to decide prior to the buckling analysis whether or not it was necessary to include coupling.

Whitney and Leissa [12] have given closed form solution for simply supported antisymmetric cross-ply plates having S-2 type boundary conditions and simply supported antisymmetric angle-ply laminates having S-3 type boundary conditions.

Jones [13] discussed the symmetrically laminated odd regular angle ply alternating in the sequence $+\theta, -\theta, +\theta, \dots, +\theta$. Here the bending-twisting coefficients D_{16} and D_{26} are the largest for small number of plies and become smaller relative to other coefficients as N is increased.

Wittrick [14] achieved exceedingly complex solution in symmetric angle plates for infinite strips in SSSS, SCSC, SFSF, CCCC boundary conditions.

Reissner and Stavsky [15] included bending-stretching effect in antisymmetrical angle ply plates. He showed that the buckling load is reduced due to coupling which is the strongest when only a small number of plies are used and decreases as N increases.

Ashton [16] suggested an approximate theory involving unsymmetric laminates. However it is found that this theory was not accurate for all problems.

Barwey [17] has made an attempt to achieve specially orthotropic behaviour of antisymmetric cross and angle ply hybrid composite laminates taking fibre orientations and thicknesses as design variables. He has shown that at optimum point laminate tends to decouple. He used Galerkin's procedure for solving the buckling problem.

Sharma and Iyengar [18] developed an exact solution procedure incorporating the coupling effect by combining the three governing equations of classical plate theory to a single eighth order partial differential equation. He took Levy's type of boundary conditions and converted partial differential equation to eighth order ordinary differential equation and then to a eighth order algebraic equation. He obtained eight by eight determinant after substituting the assumed general solution in eight homogeneous boundary conditions along the rectangular edges. The uniaxial buckling load has been found by a trial and error procedure after equating the whole determinant to zero.

Whitney [19] using the Fourier series approach studied the effect of boundary conditions upon the frequency of free vibration of an unsymmetrically laminated rectangular plate.

Bert and Mayberry [20] studied the free vibration of unsymmetrically laminated anisotropic plates with all clamped edges. He used Rayleigh Ritz procedure for finding the solution

Lin and King [21] studied the free transverse vibrations of unsymmetrically laminated plates. He solved for various boundary conditions using Bolotin asymptotic method. The method is applicable only if the governing equation can be satisfied by products of trigonometric functions in spatial coordinates paralleling the edges of rectangular region. The approximation to an eigen function is expressed as the sum of a generating solution and several corrective solution each of which is of local significance and depends upon local boundary conditions. When one or more edges are free the method is suspectful.

Kamal and Durvasula [22] made a detailed study of antisymmetric cross and angle ply laminates with fully clamped boundary condition. He also studied the effect of thickness ratios in the analysis. He used Rayleigh Ritz technique for the analysis.

Saxena [23] employed Galerkin's technique for the optimal design of hybrid composite antisymmetric laminated plates under inplane loading. He showed that in the absence of shear load, convergence has been achieved with $m = 1$ and

Reddy & Chao [24] made a comparison study of closed form and finite element solutions of thick antisymmetric angle ply laminated plates. He solved the buckling problems with all edges simply supported and all clamped boundary conditions.

1.3. LIMITATIONS OF EARLIER METHODS

- (a) Galerkin's technique by Saxena [23] requires considerable computational time. The programming part is lengthy and chances of committing errors are also more.
- (b) Rayleigh-Ritz technique by Kamal & Durvasula [22] has the same limitations of Galerkin's technique. This technique is also not that accurate when compared to Galerkin's technique as the displacement functions to be selected satisfy only the Geometric boundary conditions. For better convergence a large number of series terms are required.
- (c) Finite difference method by Hoingner & Stein [9] requires the discretization of the plate into various mesh sizes. The accuracy of the solution depends on the mesh size and smaller mesh size leads to large number of algebraic equations solving.
- (d) Finite element method by Reddy & Chao [24] has less limitation but it cannot be efficiently applied to the analysis as it requires lot of computer storage capacity depending on the number of elements used.

e. Bolotin's asymptotic method employed by Lin and King [11] has considerable computational difficulty and the method is suspectable when one or any of the rectangular edges of the plate happened to be free.

f. Closed form solution technique by Jones [13] is limited to simply supported boundary conditions of composite laminates.

g. Exact solution technique developed by Sharma [18] requires the solving of eight by eight determinant by trial and error procedure in thin antisymmetric angle ply laminates. In optimisation problem the analysis has to be repeated for parameters like fibre orientations, volume fractions etc. Overall computer time will be increased at the final stage.

There are many more methods available in the literature for the analysis of composite plates but hardly any author has used successive iteration method for the analysis of composite plates. Keeping in view over the limitations of the conventional methods, the application of successive iteration method has been investigated in detail in the present study.

1.4 SCOPE OF THE PRESENT WORK:

A study has been made using successive iteration technique to the analysis of thin decoupled and coupled antisymmetric angle ply laminates. The method can be applied to the cases to which Levy's method is applicable, i.e. boundary conditions and loadings are such that, governing set of partial differential equations reduce to a

set of ordinary differential equations. This puts some restriction on boundary conditions and nature of the laminate. Two of the edges which are opposite to each other must be simply supported and others can be of any combination. Levy's type of solution is possible for antisymmetric angle ply laminates. Antisymmetric laminates are considered in the present investigation as they possess greater flexibility with respect to design parameters.

In this study $(\dots \theta | -\theta | \theta | -\theta \dots)$ antisymmetric angle ply laminate is chosen as optimization studies [17] reveal that $(\dots -\theta | \theta_2 | -\theta_3 / \theta_3 | -\theta_2 | \theta \dots)$ type of antisymmetric laminate does not lead to any significant increase in load carrying capacity.

The method presented can be applied in principle to all types of plate problems - bending, buckling and vibration for which the number of independent variables in the governing equations can be reduced to one. Out of these, relatively more difficult to solve are eigen value problems. Detailed investigation here is restricted to eigen value problems. Biaxial buckling and free vibration problems have been investigated in detail. The necessity to undertake such a study in thin coupled composite laminates is to extend the application of successive iteration technique to the analysis of higher order shear deformable decoupled composite plates if the technique works well.

A composite plate has its length to thickness ratio (a/h) more when compared to metallic plates. In the plate analysis the effect of shear deformation is felt when (a/h) is less than 20. For $a/h < 20$, the effect of shear deformation cannot be ignored. Higher order theory developed from variational principle by J.N. Reddy [25] leads to a set of 5 sets of governing partial differential equations in five displacement variables u , v , w , Ψ_x and Ψ_y . In antisymmetric angle ply laminates it is possible to eliminate the decoupling coefficients B_{16} , B_{26} , E_{16} and E_{26} by suitably manipulating thickness and stacking sequence. The problem thus reduces to the solution of a set of 3 governing equations whose basic nature is the same as that for coupled laminate using classical plate theory.

In Chapter II of the present work, expressions are given to generate laminae properties from fibre and matrix properties. The governing differential equations for buckling and free vibration of rectangular laminates plates are presented. The boundary conditions are considered with x edges simply supported and y edges simply supported (SS), simply supported-clamped (SC), clamped-clamped (CC), clamped-free (CF), simply supported-free (SF) and free-free (FF). The development of successive iteration method to the analysis of composite plates has been discussed. Analytical expressions are given, which ensure decoupling in six layered antisymmetric angle ply-laminates.

In Chapter III, an attempt has been made to solve biaxial buckling and free vibration problems of decoupled laminates, using this method. All the boundary conditions given above are considered.

In Chapter IV, investigation has been made to apply the method to the buckling analysis of coupled laminate with x edges simply supported and y edges clamped condition. Various computational model schemes have been tried with three and two dependent variables.

CHAPTER - II

GENERAL ANALYSIS OF COMPOSITE PLATES

A study has been made to apply successive iteration technique to the analysis of composite laminates. As decoupled antisymmetric angle ply laminates are involved in this study, expressions for decoupling thickness ratios are presented in this chapter.

2.1 ASSUMPTIONS IN THIS COMPOSITE PLATE THEORY

The laminated plate analysis is based on the following assumptions as stated by Jones[13] as

- a. Each layer is orthotropic, linearly elastic and of constant thickness.
- b. Thickness of the plate is very small compared to its length and width.
- c. Body forces are absent.
- d. The displacements u , v , w in x , y and z directions respectively are small compared to the plate thicknesses.
- e. Strains ϵ_x , ϵ_y and ϵ_{xy} are small compared to unity.
- f. The plate is in a state of plane stress.
- g. Transverse shear deformation is neglected.
- h. Rotary inertial terms are neglected.

2.2 ANALYSIS

Consider a N-layered laminate as shown in Fig. 2.1. Each layer, made of continuous fibre reinforced material, considered to be orthotropic with uniform material properties E_1 , E_2 , G_{12} and ν_{12} . The subscripts 1 and 2 refer to the axes along and perpendicular to the fibre direction respectively as shown in Fig. 2.2. For such a laminate stress-strain relationship of any individual layer is expressed by Jones[13] as

$$\begin{bmatrix} \sigma_1 \\ \sigma_2 \\ \sigma_{12} \end{bmatrix} = \begin{bmatrix} Q_{11} & Q_{12} & 0 \\ Q_{12} & Q_{22} & 0 \\ 0 & 0 & Q_{66} \end{bmatrix} \begin{bmatrix} \epsilon_1 \\ \epsilon_2 \\ \epsilon_{12} \end{bmatrix} \quad (2.1)$$

where Q_{ij} are the reduced stiffnesses

$$\begin{aligned} Q_{11} &= \frac{E_1}{(1 - \nu_{12} \nu_{21})} \\ Q_{12} &= \frac{\nu_{21} E_1}{(1 - \nu_{12} \nu_{21})} = \frac{\nu_{12} E_2}{(1 - \nu_{12} \nu_{21})} \\ Q_{66} &= G_{12} \\ Q_{22} &= \frac{E_2}{(1 - \nu_{12} \nu_{21})} \end{aligned} \quad (2.2)$$

The Poisson's ratio can be obtained from the relation

If the fibres in a lamina lie at an angle θ to the x-axis of reference plane, Fig. 2.3, then the transformed stiffness matrix for the K-th lamina is given by,

$$\bar{Q}_{ij} = \begin{bmatrix} \bar{Q}_{11} & \bar{Q}_{12} & \bar{Q}_{16} \\ \bar{Q}_{12} & \bar{Q}_{22} & \bar{Q}_{26} \\ \bar{Q}_{16} & \bar{Q}_{26} & \bar{Q}_{66} \end{bmatrix} \quad (2.4)$$

where,

$$\begin{aligned} \bar{Q}_{11} &= Q_{11} \cos^4 \theta + 2(Q_{12} + 2Q_{66}) \sin^2 \theta \cos^2 \theta + Q_{22} \sin^4 \theta \\ \bar{Q}_{12} &= (Q_{11} + Q_{22} - 4Q_{66}) \sin^2 \theta \cos^2 \theta + Q_{12} (\sin^4 \theta + \cos^4 \theta) \\ \bar{Q}_{22} &= Q_{11} \sin^4 \theta + 2(Q_{12} + 2Q_{66}) \sin^2 \theta \cos^2 \theta + Q_{22} \cos^4 \theta \\ \bar{Q}_{16} &= (Q_{11} - Q_{12} - 2Q_{66}) \sin \theta \cos^3 \theta + (Q_{12} - Q_{22} + 2Q_{66}) \sin^3 \theta \\ \bar{Q}_{26} &= (Q_{11} - Q_{12} - 2Q_{66}) \sin^3 \theta \cos \theta + (Q_{12} - Q_{22} + 2Q_{66}) \sin \theta \\ \bar{Q}_{66} &= (Q_{11} + Q_{22} - Q_{12} - 2Q_{66}) \sin^2 \theta \cos^2 \theta + Q_{66} (\sin^4 \theta + \cos^4 \theta) \end{aligned} \quad (2.5)$$

From eqns. (2.5), it is evident that in a lamina with fibre oriented at $-\theta$ to x axis having identical properties, all the elements \bar{Q}_{ij} remains the same except \bar{Q}_{16} and \bar{Q}_{26} which differ only in sign.

Mathematically,

$$(\bar{Q}_{ij})_{-\theta} = -(\bar{Q}_{ij})_{\theta}, \quad i = 1, 2 \quad j = 6$$

and

Using Kirchoff's laws & thin plate hypothesis with usual notations, the following constitutive relations obtained by Jones[13]

$$\begin{bmatrix} N_x \\ N_y \\ N_{xy} \\ M_x \\ M_y \\ M_{xy} \end{bmatrix} = \begin{bmatrix} A_{11} & A_{12} & A_{16} & B_{11} & B_{12} & B_{16} \\ A_{12} & A_{22} & A_{26} & B_{12} & B_{22} & B_{26} \\ A_{16} & A_{26} & A_{66} & B_{16} & B_{26} & B_{66} \\ B_{11} & B_{12} & B_{16} & D_{11} & D_{12} & D_{16} \\ B_{12} & B_{22} & B_{26} & D_{12} & D_{22} & D_{26} \\ B_{16} & B_{26} & B_{66} & D_{16} & D_{26} & D_{66} \end{bmatrix} \begin{bmatrix} \epsilon_x \\ \epsilon_y \\ \epsilon_{xy} \\ \kappa_x \\ \kappa_y \\ \kappa_{xy} \end{bmatrix} \quad (2.7)$$

where,

$$\epsilon_x = u, x ; \epsilon_y = u, y ; \epsilon_{xy} = (u, y + v, x) ; \kappa_x = -w, xx ;$$

$$\kappa_y = -w, yy \text{ and } \kappa_{xy} = -2w, xy \text{ are the strains and}$$

$$N_x, N_y, N_{xy}, M_x, M_y, M_{xy} \text{ are the stress resultants.}$$

The extensional coupling and bending stiffnesses which are expressed as A_{ij} , B_{ij} and D_{ij} respectively are

$$\bar{A}_{ij} = \sum \bar{Q}_{ij} (z_K - z_{K-1}) \quad (2.8a)$$

$$\bar{B}_{ij} = \sum \bar{Q}_{ij} (z_K^2 - z_{K-1}^2) \quad (2.8b)$$

$$\bar{D}_{ij} = \sum \bar{Q}_{ij} (z_K^3 - z_{K-1}^3) \quad (2.8c)$$

For the antisymmetric angle ply laminates that are used in the present study

$$A_{16} = A_{26} = B_{16} = B_{26} = D_{16} = D_{26} = 0$$

using strain displacement relations, eqn. (2.7) can be rewritten for antisymmetric angle ply laminates as

$$\begin{aligned} N_x &= A_{11} u_{,x} + A_{12} v_{,y} - B_{11} w_{,xx} - B_{12} w_{,yy} \\ N_y &= A_{12} u_{,x} + A_{22} v_{,y} - B_{12} w_{,xx} - B_{22} w_{,yy} \\ N_{xy} &= A_{66} (u_{,y} + v_{,x}) - 2B_{66} w_{,xy} \\ M_x &= B_{11} u_{,x} + B_{12} v_{,y} - D_{11} w_{,xx} - D_{12} w_{,yy} \\ M_y &= B_{12} u_{,x} + B_{22} v_{,y} - D_{12} w_{,xx} - D_{22} w_{,yy} \\ M_{xy} &= B_{66} (u_{,y} + v_{,x}) - 2D_{66} w_{,xy} \end{aligned} \quad (2.9)$$

Putting $\xi = x/a$; $\eta = y/b$ and defining length to total thickness ratio as $r = a/h$, aspect ratio as $p = a/b$ eqn. (2.9) becomes

$$\begin{aligned} N_\xi &= \bar{A}_{11} \left(\frac{1}{r}\right) u_{,\xi} + \bar{A}_{12} \left(\frac{p}{r}\right) v_{,\eta} - \bar{B}_{11} \left(\frac{1}{r^2}\right) w_{,\xi\xi} - \bar{B}_{12} \left(\frac{p}{r}\right)^2 w_{,\eta\eta} \\ N_\eta &= \bar{A}_{12} \left(\frac{1}{r}\right) u_{,\xi} + \bar{A}_{22} \left(\frac{p}{r}\right) v_{,\eta} - \bar{B}_{12} \left(\frac{1}{r^2}\right) w_{,\xi\xi} - \bar{B}_{22} \left(\frac{p}{r}\right)^2 w_{,\eta\eta} \\ N_{\xi\eta} &= \bar{A}_{66} \left(\left(\frac{p}{r}\right) u_{,\eta} + \left(\frac{1}{r}\right) v_{,\xi}\right) - 2\bar{B}_{66} \left(\frac{p}{r^2}\right) w_{,\xi\eta} \end{aligned}$$

$$\begin{aligned}
M &= h (\bar{B}_{11} \left(\frac{1}{r}\right) u_{,\epsilon} + \bar{B}_{12} \left(\frac{p}{r}\right) v_{,\eta} - \bar{B}_{11} \left(\frac{1}{r^2}\right) w_{,\epsilon\epsilon} - \bar{B}_{12} \left(\frac{p}{r}\right)^2 w_{,\eta\eta}) \\
M &= h (\bar{B}_{12} \left(\frac{1}{r}\right) u_{,\epsilon} + \bar{B}_{22} \left(\frac{p}{r}\right) v_{,\eta} - \bar{D}_{12} \left(\frac{1}{r^2}\right) w_{,\epsilon\epsilon} - \bar{D}_{22} \left(\frac{p}{r}\right)^2 w_{,\eta\eta}) \\
M &= h (\bar{B}_{66} \left(\frac{p}{r}\right) u_{,\eta} + \left(\frac{1}{r}\right) v_{,\epsilon} - 2\bar{D}_{66} \left(\frac{p}{r^2}\right) w_{,\epsilon\eta})
\end{aligned}
\tag{2.10}$$

2.3 GOVERNING EQUATIONS OF ANTISYMMETRIC ANGLE PLY LAMINATES

Governing equations for biaxial buckling and vibration

as stated by Jones [13] as

$$A_{11} u_{,xx} + A_{66} u_{,yy} + (A_{12} + A_{66}) v_{,xy} - 3B_{16} w_{,xxy} - B_{26} w_{,yyy} = 0 \tag{2.11a}$$

$$(A_{12} + A_{66}) u_{,xy} + A_{66} v_{,xx} + A_{22} v_{,yy} - B_{16} w_{,xxx} - 3B_{26} w_{,xyy} = 0 \tag{2.11b}$$

$$\begin{aligned}
&D_{11} w_{,xxxx} + 2(D_{12} + 2D_{66}) w_{,xxyy} + D_{22} w_{,yyyy} - B_{16}(3u_{,xxy} + v_{,xxx}) \\
&- B_{26}(u_{,yyy} + 3v_{,xyy}) + \bar{N}_x w_{,xx} + \bar{N}_y w_{,yy} + \rho w_{,tt} = 0
\end{aligned}
\tag{2.11c}$$

Figure 2.4 shows the loading and geometry of the laminate. For free vibration problem, in the above equation, set $\bar{N}_x = \bar{N}_y = 0$ and for buckling problems set $\rho w_{,tt} = 0$. Eqn. 2.11 can be rewritten in non-dimensional form as

$$\bar{A}_{11} r u_{,\epsilon\epsilon} + \bar{A}_{66} p^2 r u_{,\eta\eta} + (\bar{A}_{12} + \bar{A}_{66}) p r v_{,\epsilon\eta} - 3\bar{B}_{16} p w_{,\epsilon\epsilon\eta} - \bar{B}_{26} p^3 w_{,\eta\eta\eta} = 0 \tag{2.12a}$$

$$(\bar{A}_{12} + \bar{A}_{66}) r p u_{,\epsilon\eta} + \bar{A}_{22} r^2 p^2 v_{,\eta\eta} + \bar{A}_{66} r v_{,\epsilon\epsilon} - 3\bar{B}_{26} p^2 w_{,\epsilon\eta\eta}$$

$$\begin{aligned}
& -3\bar{B}_{16} \rho p u_{,\xi\xi\eta} - \bar{B}_{26} \rho p^3 u_{,\eta\eta\eta} - 3\bar{B}_{26} \rho p^2 v_{,\xi\eta\eta} - \bar{B}_{16} \rho v_{,\xi\xi\xi} + \bar{D}_{11} \\
& + 2(\bar{D}_{12} + 2\bar{D}_{66})p^2 w_{,\xi\xi\eta\eta} + \bar{D}_{22} p^4 w_{,\eta\eta\eta\eta} + \lambda(w_{,\xi\xi} + K p^2 w_{,\eta\eta}) - \lambda(w)
\end{aligned}
\tag{2.12c}$$

where,

$$\lambda = \frac{N_x b^2}{E_2 h^3} \quad \text{and} \quad \lambda = \frac{\rho a^2 b^2 \omega^2}{E_2 h^3}; \quad K = \frac{N_y}{N_x}$$

For buckling problem $\lambda_f = 0$ and for free vibration problem $\lambda = 0$ in (2.12c).

2.4 BOUNDARY CONDITIONS OF ANTISYMMETRIC ANGLE PLY LAMINATES

The governing eqns. (2.12) are solved for the following boundary conditions as furnished by Jones [13]. Boundary condition on x edges in all the cases under investigation are simply supported and on y edges six combinations are investigated on x edges,

SIMPLY SUPPORTED-SIMPLY SUPPORTED

$$\text{at } \xi = 0, 1$$

$$u = w = M_\xi = N_{\xi\eta} = 0$$

2.4.1 SIMPLY SUPPORTED-SIMPLY SUPPORTED (S-S)

$$\text{at } \eta = 0, 1$$

(2.13a)

$$v = w = M_\eta = N_{\xi\eta} = 0$$

2.4.2 SIMPLY SUPPORTED-CLAMPED (S-C)

$$\begin{aligned}
 &\text{at } \eta = 0 \\
 &v = w = M_{\eta} = N_{\epsilon\eta} = 0 \\
 &\text{at } \eta = 1 \\
 &u = v = w = w_{,\eta} = 0
 \end{aligned}
 \tag{2.13b}$$

2.4.3 CLAMPED-CLAMPED (C-C)

$$\begin{aligned}
 &\text{at } = 0, 1 \\
 &u = v = w = w_{,\eta} = 0
 \end{aligned}
 \tag{2.13c}$$

2.4.4 CLAMPED-FREE (C-F)

$$\begin{aligned}
 &\text{at } \eta = 0 \\
 &u = v = w = w_{,\eta} = 0 \\
 &\text{at } \eta = 1 \\
 &N = N_{\epsilon\eta} = M = 2 M_{\epsilon\eta} + p M_{\eta,\eta} = 0
 \end{aligned}
 \tag{2.13d}$$

2.4.5 SIMPLY SUPPORTED-FREE (S-F)

$$\begin{aligned}
 &\text{at } \eta = 0 \\
 &v = w = M_{,\epsilon} = N_{\epsilon\eta} = 0 \\
 &\text{at } \eta = 1 \\
 &N_{\eta} = N_{\epsilon\eta} = M_{\eta} = 2 M_{\epsilon\eta,\epsilon} + p M_{\eta,\eta} = 0
 \end{aligned}
 \tag{2.13e}$$

2.4.6 FREE-FREE (F-F)

at $\eta = 0, 1$

$$N_{\eta} = N_{\epsilon\eta} = M_{\eta} = 2M_{\epsilon\eta,\epsilon} + p M_{\eta,\eta} = 0 \quad (2.13f)$$

2.5 LEVY'S SOLUTION PROCEDURE

The boundary conditions considered in the present study are simply supported on x edges. The displacement functions u, v, w can be assumed in a form which when substituted in eqns. (2.12), reduce these equations to a set of ordinary differential equations.

Assuming,

$$u = u(\eta) \sin \alpha \xi \text{ where } \alpha = m\pi \text{ and } m \text{ is a natural number} \quad (2.14a)$$

$$v = v(\eta) \cos \alpha \xi \quad (2.14b)$$

$$w = w(\eta) \sin \alpha \xi \quad (2.14c)$$

Substituting these expressions in (2.12) one gets the following set of ordinary differential equations

$$e_1 w^{IV} + e_2 w'' + e_3 w + e_4 v'' + e_5 v + e_6 u''' + e_7 u' = 0 \quad (2.15a)$$

$$e_8 w'' + e_9 w + e_{10} v'' + e_{11} v + e_{12} u' = 0 \quad (2.15b)$$

$$e_{13} w''' + e_{14} w' + e_{15} v' + e_{16} u' + e_{17} u = 0 \quad (2.15c)$$

where

$$e_1 = \bar{D}_{22} p^4; e_2 = -(2(D_{12} + 2\bar{D}_{66})) p^2 + Kp^4 \lambda;$$

$$e_3 = \bar{D}_{11} \alpha^4 - \lambda \alpha^2 p^2 - \lambda_{\#} p^2;$$

$$e_4 = 3\bar{B}_{26} \alpha r p^2; e_5 = -B_{16} \alpha^3 r; e_6 = -B_{26} r p^3;$$

$$e_7 = 3\bar{B}_{16} \alpha^2 r p; e_8 = -3\bar{B}_{26} \alpha p^2; e_9 = \bar{B}_{16} \alpha^3;$$

$$e_{10} = \bar{A}_{22} p^2 r; e_{11} = -\bar{A}_{66} \alpha^2 r; e_{12} = (\bar{A}_{12} + \bar{A}_{66}) \alpha r p;$$

$$e_{13} = -\bar{B}_{26} p^3; e_{14} = 3\bar{B}_{16} \alpha^2 p; e_{15} = (\bar{A}_{12} + \bar{A}_{66}) (-\alpha) r p;$$

$$e_{16} = \bar{A}_{66} p^2 r; e_{17} = -\bar{A}_{11} \alpha^2 r \quad (2.15d)$$

It may be noted that for free vibration problems $\lambda = 0$ and for buckling problems $\lambda_{\#} = 0$ in the above equation.

2.6 DEVELOPMENT OF THE SOLUTION TECHNIQUE

Writing eqns. (2.15) in the form

$$w^{IV} = f(w'', w, v'', v, u''', u') \quad (2.15e)$$

$$v'' = g(w'', w, v, u') \quad (2.15f)$$

$$u''' = s(w''', w', v', u) \quad (2.15g)$$

and integrating eqn. (2.15e) four times, eqn. (2.15f) twice, eqn. (2.5g) twice one gets expression for $w, \eta\eta\eta, w, \eta\eta, w, \eta, v, \eta, v, u, \eta, u$. These relations will involve eight constants of integration which can be determined from the eight boundary

conditions. Starting from some initially chosen functions u , v and w it is possible to develop an iterative procedure to determine the solution.

As the governing equations and associated boundary conditions are homogeneous, displacements are indeterminate with a scalar multiplier, one can arbitrarily fix a normalisation condition say $w(1/2) = 1$. This condition determines the eigen value λ at each stage of iteration. However, when the solution was attempted for laminated plates iteration does not converge. It appeared that numerical instability occurred because of the eigen value assuming negative value. A detailed investigation, starting from simpler problems, was, hence, carried out.

The procedure was investigated for column-buckling problem with both ends. 1. simply supported and 2. clamped conditions. A normalisation condition of $w(1/2) = 1$ was used for finding the eigen value λ . Convergence was achieved in the iteration and the eigen value matched closely with the exact result.

The procedure was then investigated for isotropic plate buckling problem where Levy's solution procedure is applicable. Problems with x edges simply supported and y edges in 1. simply supported, 2. clamped and 3. clamped-free boundary conditions were been studied, using normalisation condition $w(1/2) = 1$. Convergence of iteration was observed in the first case of boundary condition for all

aspect ratios between 0.2 to 4.5. But in the second and third case of boundary conditions oscillatory tendency in convergence with eigen value becoming negative in the iteration process was observed, for many aspect ratios.

It appears that λ must be positive at each stage of iteration to converge. To ensure this, a separate expression for λ is necessary. This can be done by obtaining expression in the form of a Rayleigh's quotient by using energy principles.

In the same isotropic plate problem cases investigations are carried out with Rayleigh's quotient λ instead of the normalisation condition. The oscillatory tendency was not noticed and the convergence of the iteration was achieved, agreeing well with the exact result for all the aspect ratios.

For laminated plates, the need of Rayleigh's quotient expression is thus confirmed.

2.7 EXPRESSION FOR THE EIGEN VALUE

The total potential energy expression for the problem under investigation is obtained from Whitney [12]

$$\begin{aligned} \pi_o = & \frac{1}{2} \int_0^b \int_0^a \left[(A_{11o} (u_{,x})^2 + 2A_{12} u_{,x} v_{,y} + A_{22} (v_{,y})^2 \right. \\ & + A_{66} (u_{,y} + v_{,x})^2 - 2B_{16} (u_{,y} w_{,xx} + v_{,x} w_{,xx} \\ & \left. + 2u_{,x} w_{,xy}) - 2B_{26} (u_{,y} w_{,yy} + v_{,x} w_{,yy} + 2v_{,y} w_{,xy}) \right] dx dy \end{aligned}$$

$$+ D_{22} (w_{,yy})^2 + 4D_{66} (w_{,xy})^2 - N_x (w_{,x})^2 - N_y (w_{,y})^2 - p \omega^2 (w)^2] dx dy \quad (2.16)$$

For buckling problem $\omega^2 = 0$ and for free vibration problem $N_x, N_y = 0$. Using the variables and , Eqn. (2.16) can be rewritten as

$$\begin{aligned} \pi_p = & \int_0^1 \int_0^1 [A_{11} (u_{,\xi})^2 r^2 + 2\bar{A}_{12} p f^2 u_{,\xi} v_{,\eta} + \bar{A}_{22} p^2 r^2 (v_{,\eta})^2 \\ & + A_{66} ((u_{,\eta})^2 p^2 + 2p u_{,\eta} v_{,\xi} + (v_{,\xi})^2 r^2 - 2\bar{B}_{16} (u_{,\eta} w_{,\xi\xi} p r \\ & + v_{,\xi} w_{,\xi\xi} + 2u_{,\xi} w_{,\xi\eta} p r) - 2\bar{B}_{26} (u_{,\eta} w_{,\eta\eta} r p^3 + v_{,\xi} w_{,\eta\eta} r p^2 \\ & + 2v_{,\eta} w_{,\xi\eta} p^2 r) + D_{11} (w_{,\xi\xi})^2 + 2\bar{D}_{12} p^2 w_{,\xi\xi} w_{,\eta\eta} \\ & + \bar{D}_{22} p^4 (w_{,\eta\eta})^2 + 4\bar{D}_{66} p^2 (w_{,\eta\xi})^2 - \lambda ((w)^2 + K p^2 (w_{,\eta})^2) \\ & - \lambda_f (p^2 (w)^2)] d\xi d\eta \quad (2.17) \end{aligned}$$

It may be rementioned that $\lambda_f = 0$ for buckling problems and $\lambda = 0$ for free vibration problems. Using expressions (2.14) for u, v and w in eqn. (2.17) one gets

$$\begin{aligned} p = & \frac{1}{2} \int_0^1 [\bar{A}_{11} \alpha^2 r^2 + 2\bar{A}_{12} p r^2 \alpha (uv') + \bar{A}_{22} p^2 r^2 (v')^2 \\ & + \bar{A}_{66} (p^2 (u')^2 - 2p \alpha (u'v) + v'^2 \alpha^2) r^2 + 2\bar{B}_{16} ((u'w) p r \alpha^2 \\ & - (vw) \alpha^3 r - 2(uw')) \alpha^2 p r + 2\bar{B}_{26} (-(u'w'') r p^3 \end{aligned}$$

$$\begin{aligned}
& + (v w'') r p^2 \alpha - 2(v' w') \alpha p^2 r + \bar{D}_{11} \alpha^4 (w)^2 - 2\bar{D}_{12} p^2 \alpha^2 \\
& (w w'') + \bar{D}_{22} (w'')^2 + 4\bar{D}_{66} (w')^2 + \lambda [-p^2 (w')^2 \\
& + K p^2 (w')^2] - \lambda_f (p^2 w^2) \} d\varepsilon d\eta \quad (2.18)
\end{aligned}$$

$$\pi_p = [U_1] + [Q_1] - \lambda_f [Q_2] \quad (2.19)$$

where $[U_1]$ is the internal strain energy component of the plate. $[Q_1]$ is the potential energy component due to the inplane load and $\lambda_f [Q_2]$ is the kinetic energy component due to vibration.

For a neutral equilibrium total potential energy is a constant. This implies that can be obtained by setting $\pi_p = 0$.

$$\text{Doing this } \lambda = -[U_1] / [Q_1] \quad (2.20a)$$

Natural frequency ω is determined from the fact that the maximum potential energy and maximum kinetic energy during an oscillation are equal. This implies

$$\lambda_f = [U_1] / [Q_2] \quad (2.20b)$$

As already mentioned the application of this technique is studied in coupled and decoupled thin antisymmetric angle ply laminates. Since decoupled laminates are used in the analysis separate analytical expression to ensure decoupling is required.

2.9 EXPRESSIONS FOR DECOUPLING THICKNESS RATIOS

Consider a ~~six~~ layered antisymmetric angle ply laminate as in Fig. 2.5. In such a laminate for every lamina oriented an angle θ above the mid plane there exists an identical lamina placed at an equal distance below the mid plane but oriented at a negative angle θ . One needs to make B_{16} and B_{26} zero for decoupling between inplane displacements u, v and transverse displacement w . For given material properties and fibre orientations of the laminae it may be possible to make B_{16} and B_{26} zero by suitably selecting the thickness ratios of the layers of a laminate. Proceeding in a similar way as Sharma [17] and Saxena [24]. Using eqn. (2.8b)

$$B_{1j} = \frac{2}{2} [\bar{Q}_{1j1} (t_3^2 - 0) + \bar{Q}_{1j2} ((t_2+t_3)^2 - t_3^2) + \bar{Q}_{1j3} ((t_1+t_2+t_3)^2 - (t_2+t_3)^2)] \quad (2.21)$$

$$\text{Let } \frac{\bar{Q}_{1j3}}{\bar{Q}_{1j1}} = \beta_{1j}, \quad \frac{\bar{Q}_{1j2}}{\bar{Q}_{1j1}} = \alpha_{1j}, \quad \frac{t_1}{t_3} = R_1, \quad \frac{t_2}{t_3} = R_2$$

Eqn. (2.21) becomes

$$\beta_{1j} + \alpha_{1j} ((1 + R_2)^2 - 1) + ((1 + R_1 + R_2)^2 - (1 + R_2)^2) = 0 \quad (2.22)$$

Let $(1 + R_2)^2 = y_1$ and $(1 + R_1 + R_2)^2 = y_2$ then

$$\beta_{1j} + \alpha_{1j} (y_1 - 1) + (y_2 - y_1) = 0$$

Solving eqn. (2.22)

$$R_2 = -\sqrt{1 + A} - 1$$

$$R_1 = \frac{-\sqrt{(1 - \alpha_{16})(1 + A)} + (\alpha_{16} - \beta_{16})}{\alpha_{16} - \beta_{16}} = \sqrt{1 + A} \quad (2.23)$$

$$\text{where } A = (\beta_{16} - \beta_{26}) / (\alpha_{26} - \alpha_{16})$$

$$\text{for } R_2 > 0; \quad A > 0 \text{ and for } R_1 > 0; \quad \frac{\beta_{16}\alpha_{26}}{\alpha_{16}\beta_{26}} < 1$$

For homogeneous laminates with alternate $+\theta$ and $-\theta$ (Fig. 2.5)

$$\beta_{ij} = 1 \text{ and } \alpha_{ij} = -1. \text{ Substituting in eqn.(2.22)}$$

$$R_2 = -(R_2 + 1) \pm \sqrt{2R_2^2 + 2R_2} \quad (2.24)$$

Any combinations of R_1 and R_2 which satisfy the above relation, decouple the laminate.

The analysis is much simpler in decoupled laminates, as the number of governing equations are reduced to one with this ratios. The application of the successive iteration technique can be studied readily in decoupled laminates.

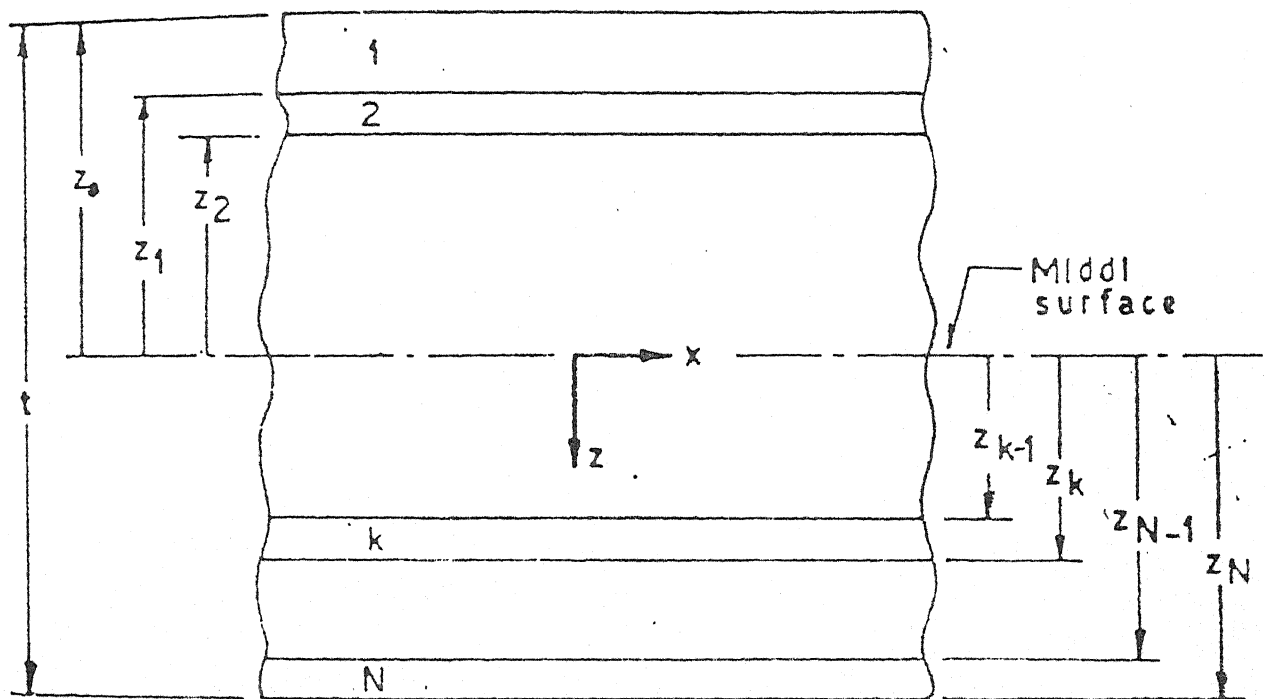


FIG. 2-1: GEOMETRY OF A n - LAYERED LAMINATE.

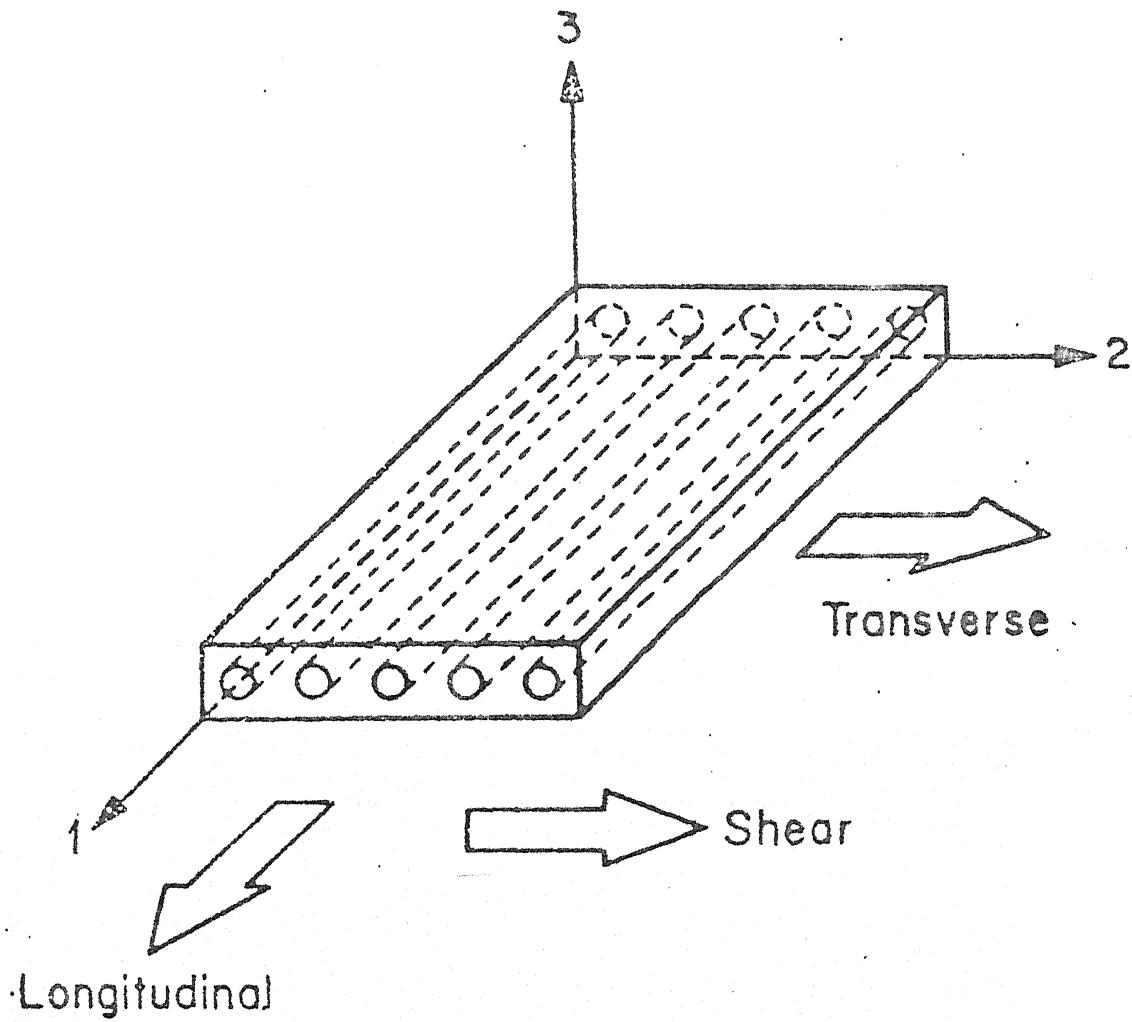


FIG 2.2 : UNIDIRECTIONALLY REINFORCED LAMINA

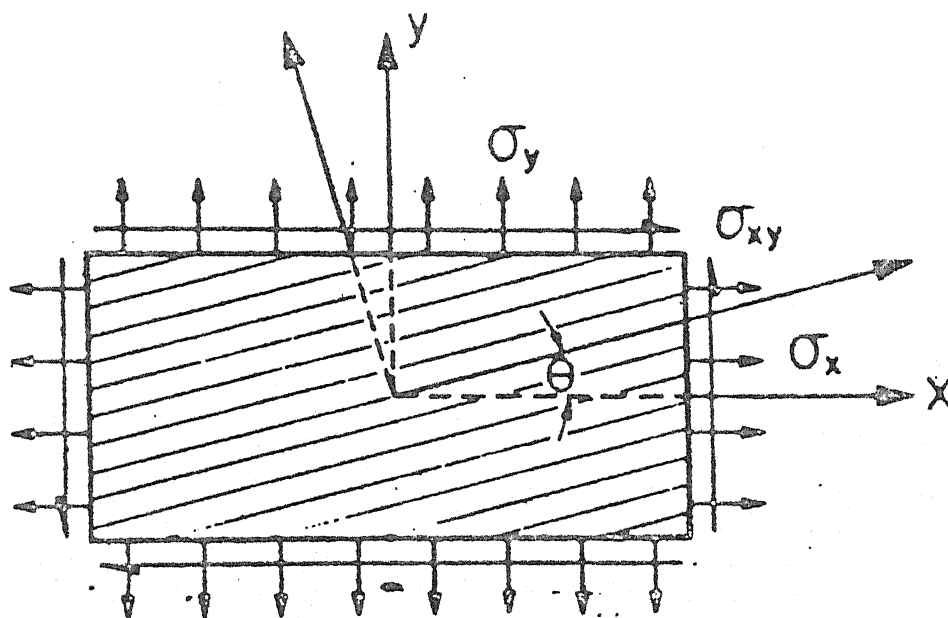


FIG. 2.3 : POSITIVE ROTATION OF LAMINA AXES
BY θ° W.R.T. LAMINATE AXES.

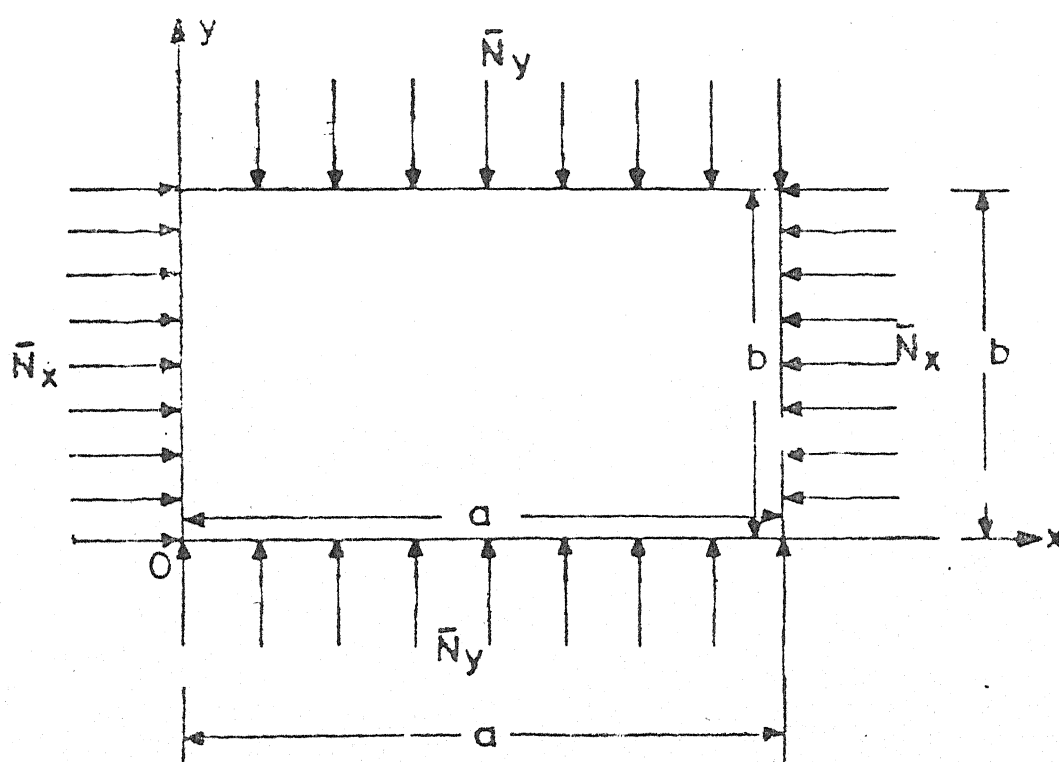
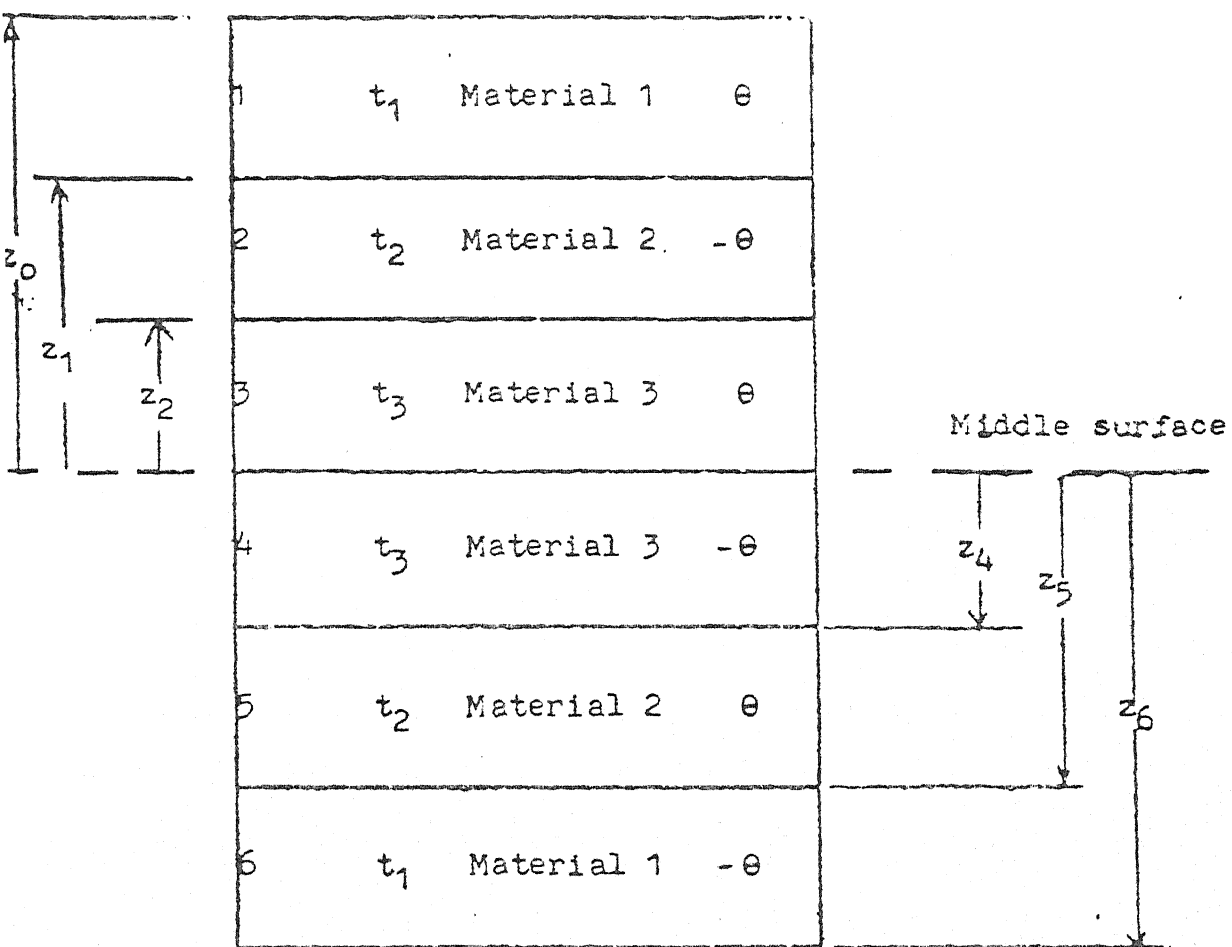


FIG. 2.4: LOADING AND GEOMETRY OF RECTANGULAR PLATE.



$$z_0 = -z_6 = -(t_1 + t_2 + t_3)$$

$$z_1 = -z_5 = -(t_2 + t_3)$$

$$z_2 = -z_4 = -t_3$$

$$z_3 = 0$$

Fig.2.5 Geometry of a six-layered laminate.

CHAPTER - III

ANALYSIS OF DECOUPLED LAMINATES

In this chapter an attempt has been made to analyse decoupled six layered antisymmetric angle ply laminates using successive iteration technique. Biaxial buckling problems are studied with x edges simply supported and y edges in combinations of (1) simply supported, (2) simply supported - clamped (S-C), (3) clamped (C-C), (4) clamped free (C-F), (5) simply supported - free (S-F), (6) free (F-F) boundary conditions. Free vibrations problems are studied with x edges simply supported and y edges in combinations of (1) simply supported (S-S), (2) clamped (C-C), (3) free (F-F) boundary conditions.

3.1 BIAxIAL BUCKLING PROBLEMS

3.1.1 GOVERNING EQUATION

Since B_{16} and B_{26} are made zero, the eqns. (2.8a,b,c) get decoupled. The eqn. (2.8c), then reduces to an equation with a single displacement variable w as

$$e_1 w^{IV} + e_2 w'' + e_3 w = 0 \quad (3.1)$$

where

$$e_1 = \bar{D}_{22} p^4; e_2 = -2(D_{12} + 2\bar{D}_{66}) \alpha^2 p^2 + K p^4 \lambda; e_3 = \bar{D}_{11}^4 - \alpha^2$$

(

Eqn. (3.1) can be rewritten as

$$w^{IV} = c_1 w + c_2 w'' \quad (3.2)$$

where

$$\begin{aligned} c_1 &= z_1 - z_2 \lambda; \quad c_2 = z_3 - z_4 \lambda; \quad z_1 = \frac{\bar{D}_{11}}{\bar{D}_{22}} \left(\frac{\alpha}{p}\right)^4; \\ z_2 &= - \frac{1}{\bar{D}_{22}} \left(\frac{\alpha}{p}\right)^2; \quad z_3 = \frac{2(\bar{D}_{12} + 2\bar{D}_{66})}{\bar{D}_{22} p^2}; \\ z_4 &= \frac{K}{\bar{D}_{22}} \end{aligned} \quad (3.2a)$$

Integrating the eqn. (3.2) successively

$$w''' = c_1 \int_0^\eta w d\eta + c_2 \int_0^\eta w' d\eta + K_1 \eta \quad (3.3a)$$

$$w'' = c_1 \int_0^\eta \int_0^\eta w d\eta^2 + c_2 w + K_1 \eta + K_2 \quad (3.3b)$$

$$w' = c_1 \int_0^\eta \int_0^\eta \int_0^\eta w d\eta^3 + c_2 \int_0^\eta w d\eta + K_1 \frac{\eta^2}{2} + K_2 \eta + K_3 \quad (3.3c)$$

$$\begin{aligned} w &= c_1 \int_0^\eta \int_0^\eta \int_0^\eta \int_0^\eta w d\eta^4 + c_2 \int_0^\eta \int_0^\eta w d\eta^2 + K_1 \frac{\eta^3}{6} \\ &+ K_2 \frac{\eta^2}{2} + K_3 \eta + K_4 \end{aligned} \quad (3.3d)$$

where K_1 , K_2 , K_3 and K_4 are the constants of integration to be determined from the boundary conditions.

3.1.2 RAYLEIGH'S QUOTIENT

Governing eqns. (2.12a,b,c) get decoupled for zero values of B_{16} and B_{26} . Eqn. (2.12c) can be repeatedly integrated to determine w and λ . Eqns. (2.12a) and (2.12b) are the coupled equations determining u and v . However these equations are homogeneous and the associated boundary conditions are also homogeneous. In the absence of any eigen parameter the solution of these equations is $u = 0$ and $v = 0$. Using these zero values for u and v in eqn. (2.18). One gets the following expression for λ from eqn. (2.20a).

$$\lambda = \frac{\int_0^1 \left[\bar{D}_{11} \left(\frac{\alpha}{p} \right)^4 w^2 - 2\bar{D}_{12} \alpha^2 w w'' + \bar{D}_{22} p^2 (w'')^2 + 4D_{66} \alpha^2 (w')^2 \right] d\eta}{\int_0^1 \left[\alpha^2 w^2 + K p^2 (w')^2 \right] d\eta} \quad (3.4)$$

3.1.3 (S+S) BOUNDARY CONDITION CASE

The boundary conditions are obtained after substituting the displacement relation (2.14c) in eqn. (2.13a) as

$$w \neq w'' = 0 \text{ at } \eta = 0, 1 \quad (3.5)$$

Let the definite integrals be defined as

$$q_1 = \int_0^1 \int_0^1 w d\eta, \quad q_2 = \int_0^1 \int_0^1 w d\eta^2, \quad q_3 = \int_0^1 \int_0^1 \int_0^1 w d\eta^3, \quad q_4 = \int_0^1 \int_0^1 \int_0^1 \int_0^1 w d\eta^4 \quad (3.6)$$

Using eqn. (3.5) in eqns. (3.3.b) and (3.3d) the constants of integration are obtained as,

$$K_1 = - (c_1 q_2 + c_2 w(1)); K_2 = 0; K_3 = - \frac{K_1}{6} - (c_1 q_4 + c_2 q_2); K_4 = 0 \quad (3.7)$$

3.1.4 STEPS IN APPLYING SUCCESSIVE ITERATION TECHNIQUE

The main steps to apply the successive iteration technique are as follows:

- i) For the given fibre and matrix properties E_1 , E_2 , G_{12} and ν_{12} generate $[Q]$ and $[\bar{Q}]$ matrices using eqn. (2.4) and eqn. (2.5) respectively.
- ii) Making use of the decoupling thickness ratios R_1 and R_2 calculate the percentage thicknesses of the layers.
- iii) For the specified geometry and thickness, compute the coefficients of the stiffness matrix \bar{D}_{1j} .
- iv) For the given aspect ratio (p) and mode number (m) calculate the constants z_1 , z_2 , z_3 and z_4 .
- v) Select some initial function $w(\eta)$ and an initial value for λ . Chosen function need not (say $w(\eta) = 1$) satisfy any boundary conditions.
- vi) Find the constants c_1 and c_2 . For the given boundary conditions of the problem evaluate the integration constants K_1 , K_2 , K_3 and K_4 . For (S-S) case find the constants from eqn. (3.7).

- vii) Evaluate the functions w_{n+1} , w'_{n+1} , w''_{n+1} from eqns. (3.3) using w_n , where suffix n denotes the iteration number.
- viii) Normalise w_{n+1} , w'_{n+1} and w''_{n+1} using the maximum value of w_n .
- ix) Find the eigen value λ from eqn. (3.4).
- x) Transfer the control to step (vi) and repeat the process until $|(\lambda_{n+1} - \lambda_n) / \lambda_{n+1}| \leq \xi$, a small number (say $\xi = 0.001$).
- xi) For various values of mode numbers, find the eigen values λ_{n+1} and the minimum out these is the buckling load.

3.1.5 CONSTANTS OF INTEGRATION

For the remaining various boundary conditions at the y edges, the constants of integration are found in a similar way as in SS case. Let the constants be defined as,

$$a_1 = - \frac{\bar{D}_{12}}{\bar{D}_{22}} \left(\frac{\alpha}{p}\right)^2, \quad a_2 = - \left(\frac{\alpha}{p}\right)^2 \frac{(\bar{D}_{12} + 4 \bar{D}_{66})}{\bar{D}_{22}},$$

$$a_3 = c_1 (a_2 + a_1 q_4) + c_2 (w(1) + a_1 q_2); \quad a_4 = c_1 (q_1 + a_2 q_3) + c_2 (w'(1) + a_2 q_1);$$

$$a_5 = \left(1 + \frac{a_1}{6}\right); \quad a_6 = \left(1 + \frac{a_2}{2}\right);$$

$$a_7 = \left(1 + \frac{a_1}{2}\right); \quad a_8 = a_1 - a_2 a_5 \quad (3.8)$$

then for various boundary conditions at y edges,

SIMPLY SUPPORTED-CLAMPED (S-C)

$$K_1 = (3 c_1 (q_4 - q_3) + c_2 (q_2 - q_1)); K_2 = 0$$

$$K_3 = c_1 (0.5 q_3 - 1.5 q_4) + c_2 (0.5 q_1 - 1.5 q_2); K_4 = 0$$

(3.9)

CLAMPED-CLAMPED (C-C)

$$K_1 = c_1 (12q_4 - 6q_3) + c_2 (12q_2 - 6q_1); K_2 = c_1 (2q_3 - 6q_4) + c_2 (2q_1 - 6q_2)$$

$$K_3 = 0; K_4 = 0$$

(3.9b)

CLAMPED-FREE (C-F)

$$K_1 = - \frac{(a_3 + a_7 K_2)}{a_5}; K_2 = \frac{(a_4 a_5 - a_3 a_7)}{(a_6 a_7 - a_2 a_5)}; K_3 = 0; K_4 = 0$$

(3.9c)

SIMPLY SUPPORTED-FREE (S-F)

$$K_1 = - \frac{(a_3 + a_1 K_3)}{a_5}; K_2 = 0; K_3 = \frac{(a_4 a_5 - a_3 a_6)}{(a_1 a_6 - a_2 a_5)}; K_4 = 0$$

(3.9d)

FREE-FREE

$$K_1 = -a_2 K_3; K_2 = - \frac{2(2a_4 a_8 + a_2^2 a_3)}{(a_1 a_2^2 + 4a_2 a_8)}; K_3 = - \frac{(2a_3 + a_1 K_2)}{2a_8};$$

$$K_4 = - \frac{K_2}{a_1}$$

(3.9e)

3.2 FREE VIBRATION PROBLEMS

The eqns. (3.2) and (3.3) are the same with the difference in values of c_1 and c_2 as

$$c_1 = z_5 - z_6 \lambda_f; \quad z_5 = - \frac{\bar{D}_{11}}{\bar{D}_{22}} \left(\frac{\alpha}{p}\right)^4; \quad z_6 = - \frac{1}{\bar{D}_{22}} \left(\frac{1}{p}\right)^2;$$

$$c_2 = \frac{2(\bar{D}_{12} + 2\bar{D}_{66})}{\bar{D}_{22}} \left(\frac{\alpha}{p}\right)^2 \quad (3.10)$$

Expression for Rayleigh's quotient is obtained in the same manner as explained in section 3.1.2,

$$\lambda_f = \frac{\int_0^1 \left[\left(\bar{D}_{11} \left(\frac{\alpha}{p}\right)^4 w^2 - 2\bar{D}_{12}^2 w w'' + \bar{D}_{22} p^2 (w'')^2 + 4\bar{D}_{66}^2 (w')^2 \right) d\eta \right]}{\int_0^1 w^2 d\eta} \quad (3.11)$$

The boundary conditions and the values of the integration constants are the same as that for the buckling problem.

The analysis has been made in (S-S), (C-C) and (F-F) boundary condition cases with successive iteration technique. The application of this technique is very similar to the buckling problem.

$\gamma_{12} = 0.25$ and CFRP are $E_1/E_2 = 6.33$, $G_{12}/E_2 = 0.667$,
 $\gamma_{12} = 0.20$. The decoupling thickness ratios of $R_1 = t_1/t_3 = 1$,
 and $R_2 = t_2/t_3 = 2.0$ are used in the analysis. The analysis
 was carried out in DEC-1090 system at I.I.T. Kanpur.

Boundary conditions SS, SC, CC, CF, SF and FF have been
 considered in biaxial problems to determine the buckling load
 $\lambda = \frac{\bar{N}_x b^2}{E_2 h^3}$, using successive iteration technique. Condition
 CC, SS and FF have been considered in the free vibration problem
 to determine the non-dimensional natural frequency $\lambda_f = ab \frac{\omega \sqrt{\rho}}{\sqrt{E_2} h^3}$
 Successive iteration technique was studied in detail and the
 eigen values obtained in the iteration process are presented in
 tabular form for different starting functions, and mesh sizes for
 quadrature using trapezoidal rule. A parametric study has been
 made to investigate the variation of buckling load (λ) and natural
 frequency (λ_f) with different fibre orientations (θ), aspect
 ratios (AR) and buckling load ratios (K).

3.4 RESULTS AND DISCUSSION

Successive iteration technique gives very good results,
 agreeing well with the results of other techniques. The present
 technique gives slightly higher values of buckling loads and
 natural frequencies compared to other exact solution techniques.
 The reason is due to the use of energy expression and discrete
 displacement functions in the analysis.

Table 3.1 shows the eigen values (λ) obtained in the
 iteration process for various aspect ratios (AR) with fibre

orientation $\theta = 30^\circ$ and buckling load ratio $K = 0$ in GFRP laminate. A mesh size of 0.01 is used with starting function $w(\eta) = 1$ and convergence criteria $\xi = 0.01$.

For $AR = 0.5, 1.0, 1.5$ and 2.0 , the buckling loads are obtained as 130.9, 79.36, 87.75 and 79.16. In most of the cases the iterations converged in not more than six iterations. The solution is obtained quickly and consumes less computational time.

Table 3.2 shows the effect of starting functions, mesh size and convergence criteria in GFRP laminate with $\theta = 30^\circ$, $AR = 1$ and $K = 0$.

- i) For a starting function $w(\eta) = 1$, mesh interval = 0.01 and convergence criteria $\xi = 0.01$, the buckling load (λ_{d_1}) is obtained as 87.75.
- ii) For a starting function $w(\eta) = \sin \pi \eta$ and with same mesh size of the above case and the buckling load (λ_{d_2}) is obtained as 87.75.
- iii) For a starting function $w(\eta) = 1$ and a mesh size = 0.001 the buckling load (λ_{d_3}) is obtained as 87.75.
- iv) For a starting function $w(\eta) = 1$, mesh size 0.01 and $\xi = 0.001$ the buckling load (λ_{d_4}) is obtained as 87.71.

3.4.1 BUCKLING PROBLEMS

All the laminates considered in the present study are GFRP except in Fig. 3.7 where CFRP is taken.

Figure 3.1 shows the λ vs. θ curves in CC, SC, SS, CF, SF and FF conditions with $K = 0$ and $AR = 1$. The curves in CC condition agrees closely with Sharma [18] and in SS condition agrees with Jones [13]. As θ increases, λ increases, reaches a maximum value of 102.3 at $\theta = 43$ in CC condition, 88.2 at $\theta = 44$ in SC condition and 68.1 at $\theta = 45$ in SS condition. In all free edge cases, as θ increases, λ decreases. λ reaches a maximum value of 34.2, 32.3 and 30.8 in CF, SF and FF conditions respectively at $\theta = 0$. It is observed that $\lambda(CC) > \lambda(SC) > \lambda(SS)$ $\lambda(CF) > \lambda(SF) > \lambda(FF)$ in the curves for all values of θ .

Figure 3.2 shows the λ vs. θ curves in CC, SC and SS conditions with $K = 1$ and $AR = 2$. The same trend as in Fig. 3.1 is observed. λ reaches a maximum value of 42.1 at $\theta = 66.1$ in CC condition, 24.4 at $\theta = 72$ in SC condition and 13.2 at $\theta = 79$ in SS condition.

Figure 3.3 shows the λ vs. AR curves in CC, SC, SS, CF, SF and FF conditions with $K = 0$ and $\theta = 30^\circ$. As the AR increases, λ decreases in all the curves upto $AR = 1.5$, and then becomes more or less constant. The maximum for CC, SC, SS, CF, SF and FF conditions are 130.9, 129.8, 114.9, 53.8, 51.8 and 12.1 respectively, occurring at $AR = 0.5$. The curve in CC condition agrees with Sharma [18].

Figure 3.4 shows the λ vs. AR curves in CC, SC, SS, CF, SF and FF conditions with $K = 1$ and $\theta = 60^\circ$. The same trends as in Fig. 3.3 is observed. The maximum λ for CC, SC, SS, CF, SF and FF conditions are 68.8, 50.9, 42.8, 21.9, 19.8 and 8.9 respectively, occurring at $AR = 0.5$.

Figure 3.5 shows the λ vs. K curves in CC, SC, SS, CF, SF and FF conditions with $\theta = 30$ and $AR = 1$. As K increases, λ decreases. The maximum λ for CC, SC, SS, CF, SF and FF conditions are 77.8, 67.9, 58.9, 28.1 and 8.8 occurring at $K = 0$ (uniaxial loading).

Figure 3.6 shows the λ vs. K curves in CC, SC, SS, CF, SF and FF conditions with $\theta = 60$ and $AR = 2$. The same trend is observed as in Fig. 3.5. The FF curve reaches almost zero value at $K = 0.5$. The maximum λ for CC, SC, SS, SF and FF conditions are for 62.1, 53.9, 44.0, 23.1, 19.90 and 9.1 occurring at $K = 0$.

Figure 3.7 shows the λ vs. AR curves in FF condition with $K = 0$ and $AR = 1$ for $\theta = 30^\circ$, 45° and 60° . The curves agree closely with Sharma 18. As AR increases λ decreases.

$\lambda(\theta = 30) > \lambda(\theta = 45^\circ) > \lambda(\theta = 60^\circ)$ is observed.

3.4.2 FREE VIBRATION PROBLEMS

Figure 3.8 shows the $\sqrt{\lambda_f}$ vs. AR curves in CC, SS and FF condition with $\theta = 30^\circ$. As AR increases, $\sqrt{\lambda_f}$ decreases upto $AR = 1.2$ in CC condition and 1.5 in SS condition. For $AR > 1.2$ in CC condition and 1.5 in SS condition $\sqrt{\lambda_f}$ increases. The minimum value of $\sqrt{\lambda_f}$ for CC and SS conditions are 33.9 and 32.8 respectively. In FF condition as AR increases $\sqrt{\lambda_f}$ value

decreases continuously from 32 at $AR = 0.5$.

Figure 3.9 shows the $\sqrt{\lambda_f}$ vs. θ curves in CC, SS and FF conditions with $AR = 1.0$. $\sqrt{\lambda_f}$ increases as θ increases and attains a maximum value of 41 at $\theta = 90^\circ$ in CC condition. In FF condition, decreasing trend is observed as θ increases. The maximum $\sqrt{\lambda_f}$ occurs at $\theta = 0$. In SS condition, symmetry is observed about $\theta = 45^\circ$ with a maximum value of $\sqrt{\lambda_f}$ as 25.8 and the curve agrees with Jones [13].

Figure 3.10 shows $\sqrt{\lambda_f}$ vs. θ curves in CC, SS and FF conditions for $AR = 2.0$. $\sqrt{\lambda_f}$ increases, as θ increases in CC condition, reaches a maximum value of $\sqrt{\lambda_f} = 82.2$ at $\theta = 90^\circ$. In SS condition as θ increases $\sqrt{\lambda_f}$ increases reaches a maximum of 36 at $\theta = 84.3$. In FF condition $\sqrt{\lambda_f}$ decreases, as θ increases with maximum $\sqrt{\lambda_f}$ occurring at $\theta = 0$.

3.5 GENERAL OBSERVATIONS

Based on the above study using successive iteration technique certain general comments can be made.

1. Successive iteration technique gives very good results agreeing well with the results of other techniques in both buckling and free vibration problems. The technique gives slightly higher values of buckling loads or natural frequency compared to other exact solution techniques. The reason is due to the use of energy expression and discrete displacement functions in the analysis.

2. The computational efficiency is quite high and in most of the cases the technique converges in just 4 or 5 iterations.
3. A mesh size of 0.01, interval is sufficient, for quadrature using trapezoidal rule, to achieve desired accuracy.
4. Convergence criteria $(| \frac{(\lambda_{n+1} - \lambda_n)}{\lambda_n} | \geq 0.01)$ is sufficient for the two successive iterations to converge.
5. In buckling problems with CC, SC and SS conditions as fibre θ increases, buckling load λ increases, reaches maximum for particular θ (optimal) and then drops. In plate with CF, SF and FF conditions λ value drops continuously as θ increases and hence it is desirable to design plate for zero degree fibre orientation to achieve optimization.
6. As the aspect ratio AR increases, λ decreases in all the boundary conditions.
7. As the buckling load ratio K increases, λ decreases. Interaction curves for biaxial loading can be drawn, which will be useful for design.

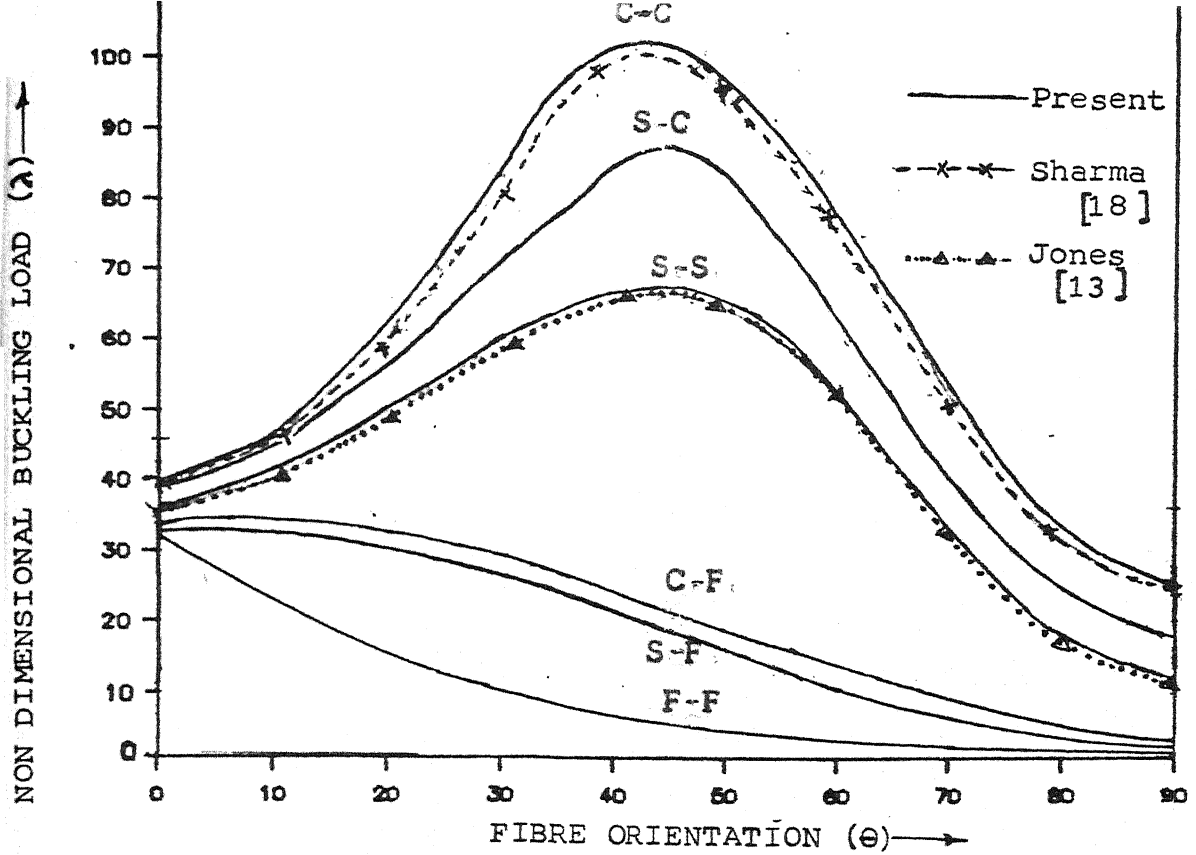


FIG.3.1 : VARIATION OF NONDIMENSIONAL BUCKLING LOAD (λ) WITH FIBRE ORIENTATION (θ) . ($K = 0.0$, $AR = 1.0$)

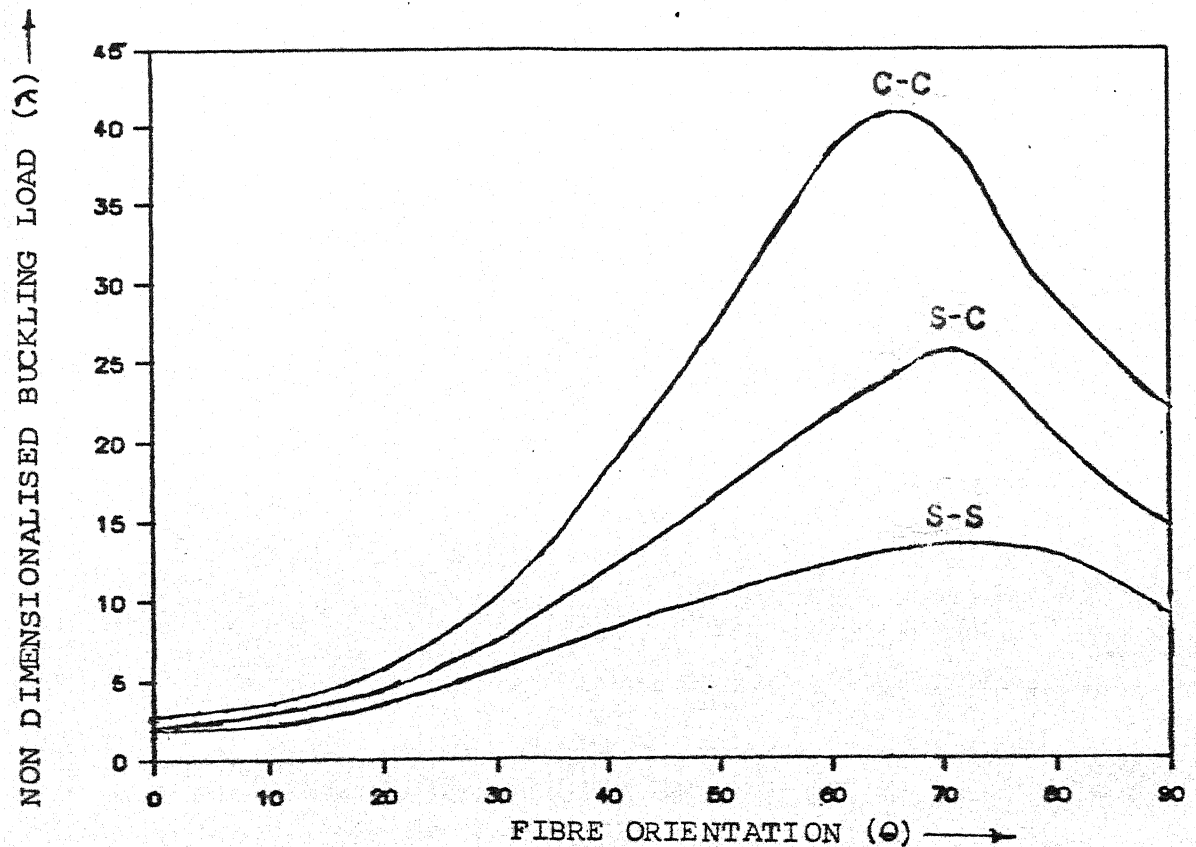


FIG. 3.2 : VARIATION OF NONDIMENSIONAL BUCKLING LOAD (λ) WITH FIBRE ORIENTATION (θ) . ($K = 2.0$, $AR = 2.0$)

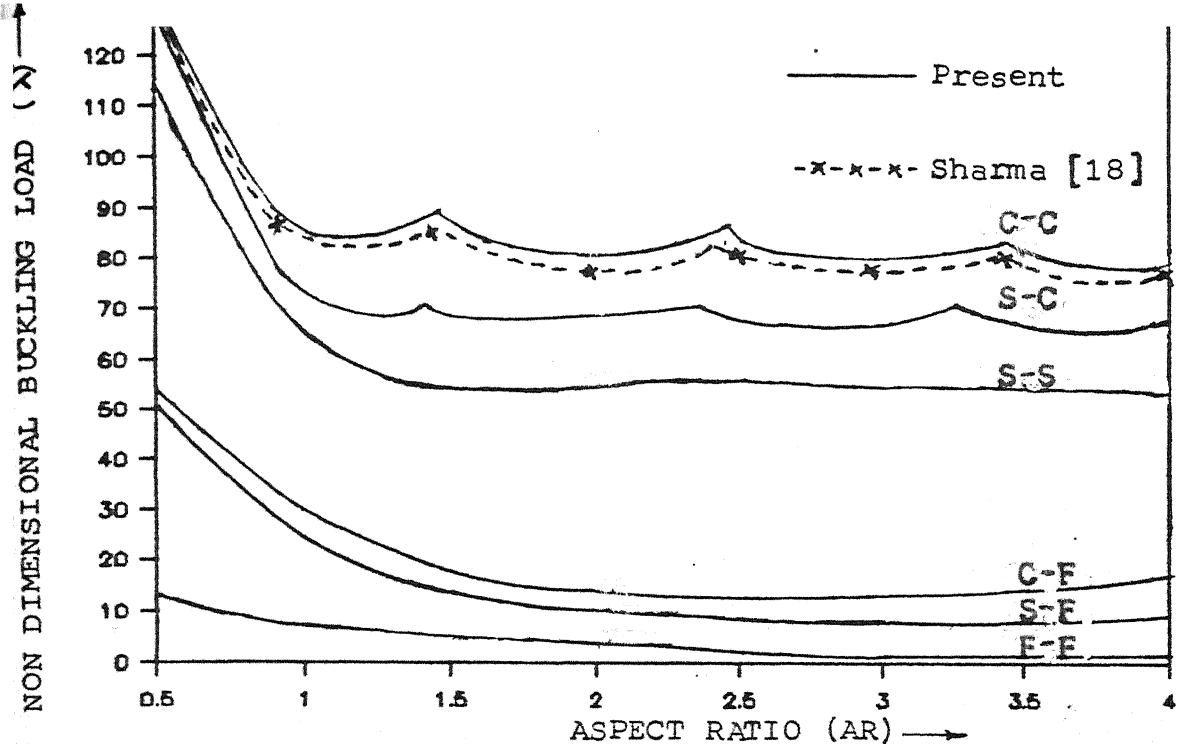


FIG.3.3 : VARIATION OF NONDIMENSIONAL BUCKLING LOAD (λ) WITH ASPECT RATIO (AR). ($K = 0.0$, $\theta = 30$)

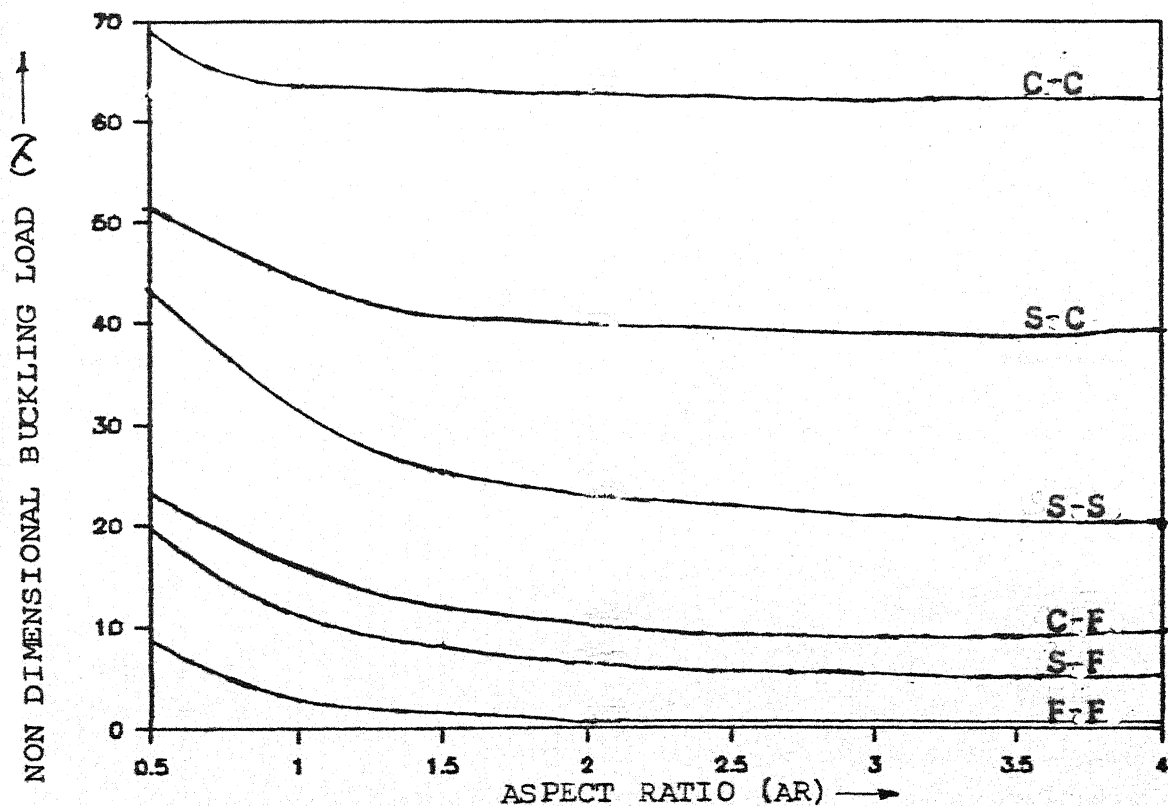


FIG.3.4 : VARIATION OF NONDIMENSIONAL BUCKLING LOAD (λ) WITH ASPECT RATIO (AR). ($K = 1.0$, $\theta = 60$)

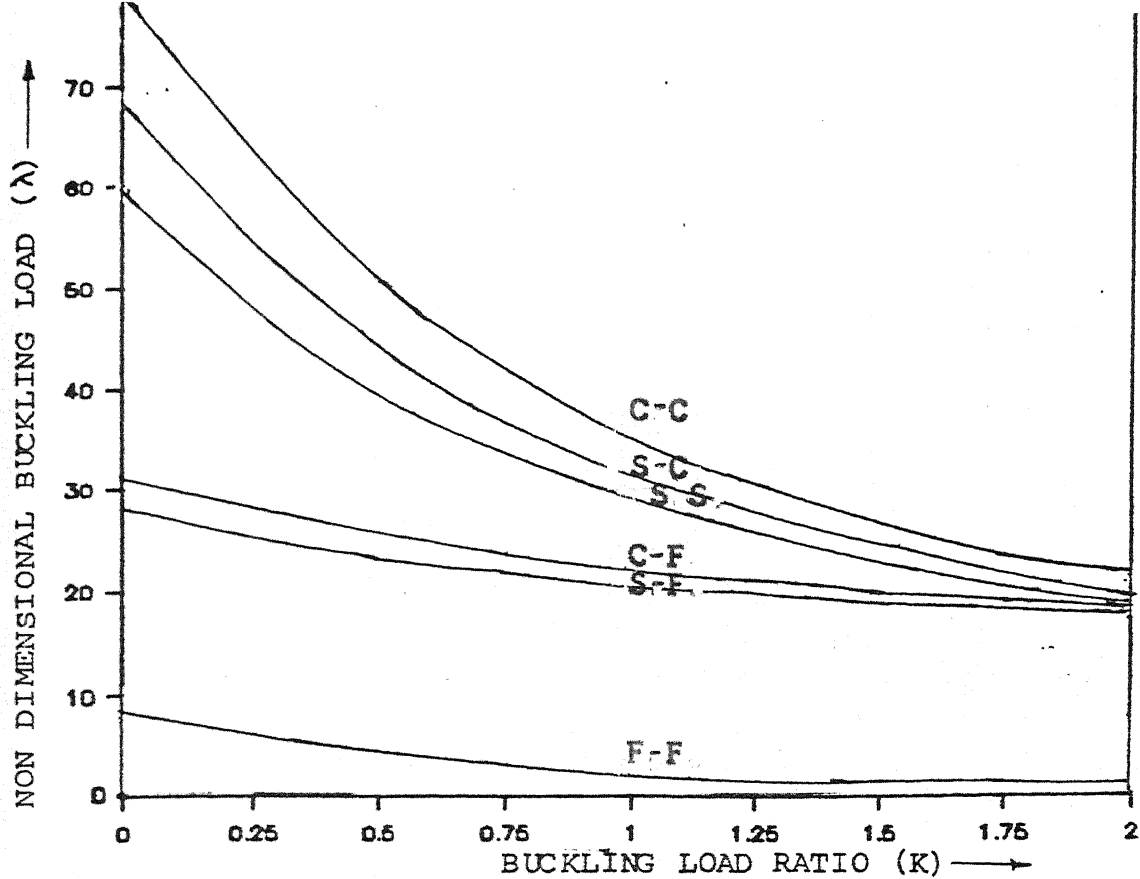


FIG.3.5 : VARIATION OF NONDIMENSIONAL BUCKLING LOAD (λ) WITH BUCKLING LOAD RATIO (K). ($AR = 1.0$, $\theta = 30^\circ$)

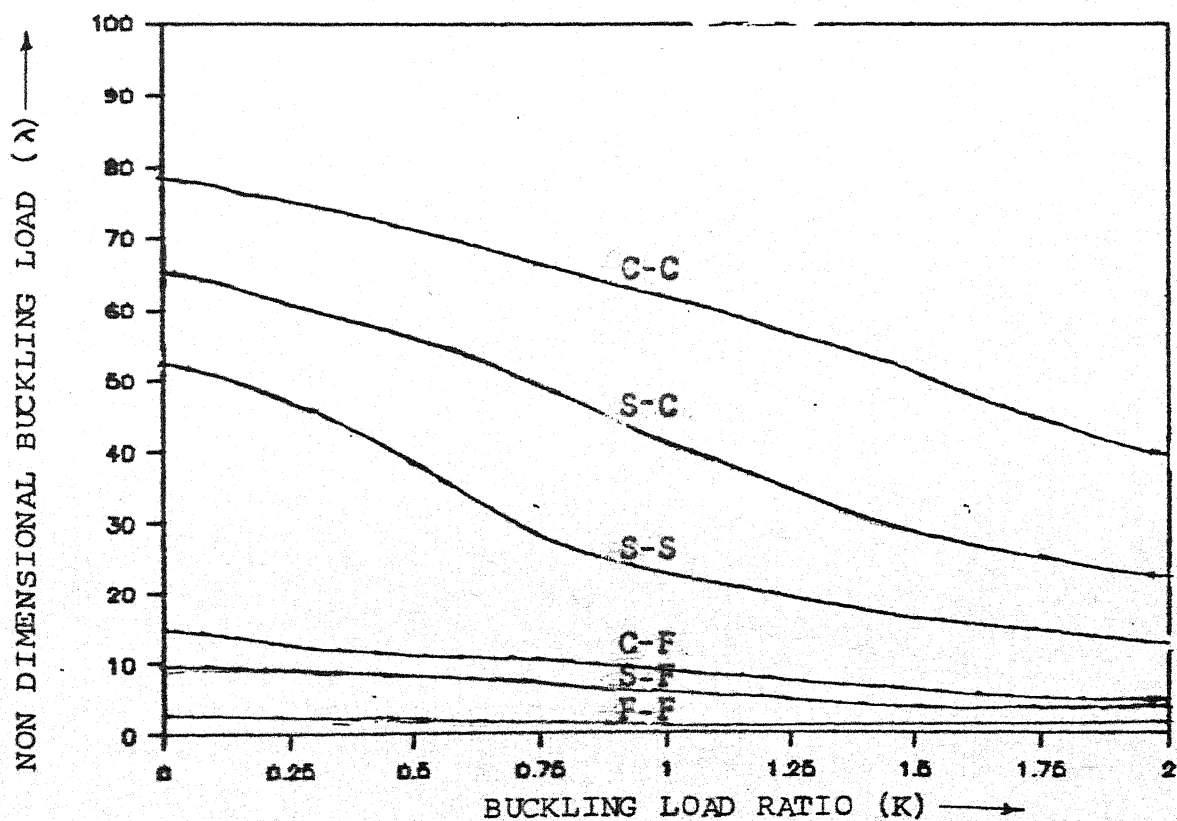


FIG.3.6 : VARIATION OF NON DIMENSIONAL BUCKLING LOAD (λ) WITH BUCKLING LOAD RATIO (K). ($AR = 2.0$, $\theta = 60^\circ$)

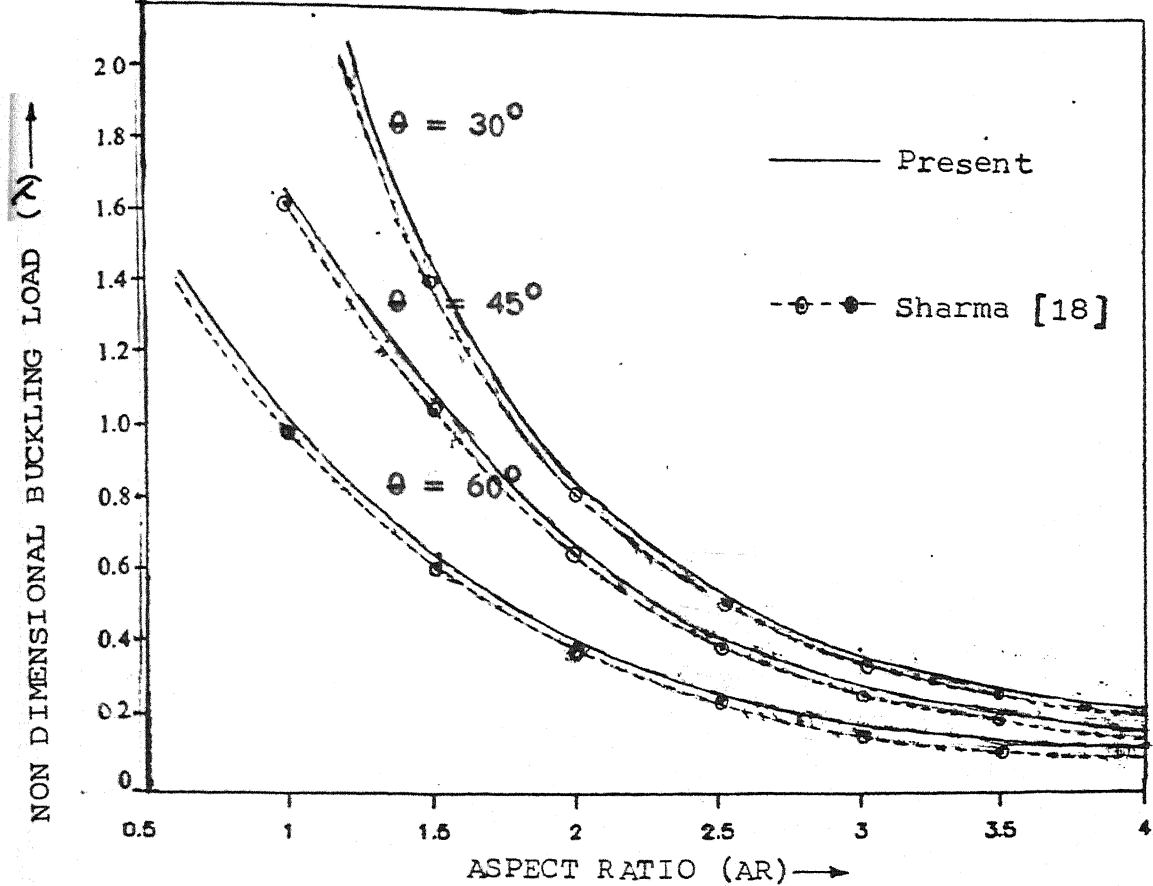


FIG.3.7 : VARIATION OF NON DIMENSIONAL BUCKLING LOAD (λ) WITH ASPECT RATIO (AR). ($K = 0.0$, $AR = 1.0$)

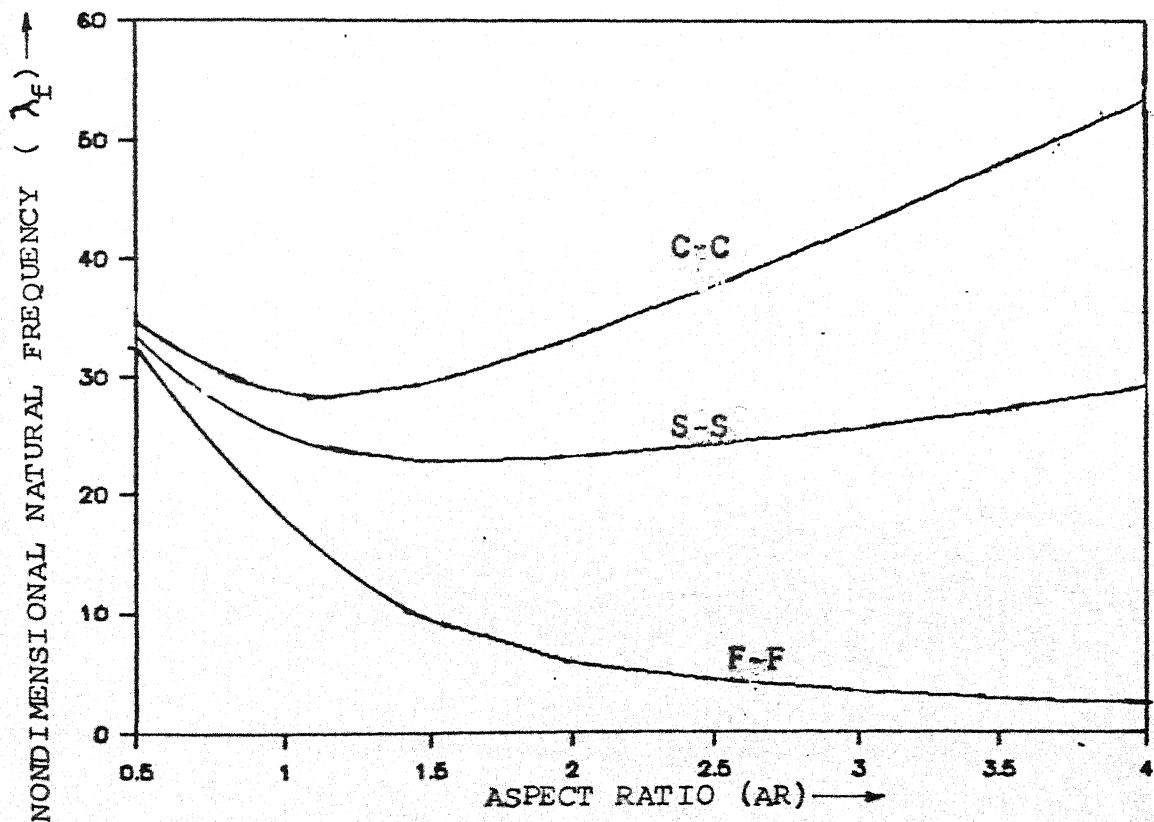


FIG.3.8 : VARIATION OF NONDIMENSIONAL NATURAL FREQUENCY (λ_F) WITH ASPECT RATIO (AR). ($\theta = 30^\circ$)

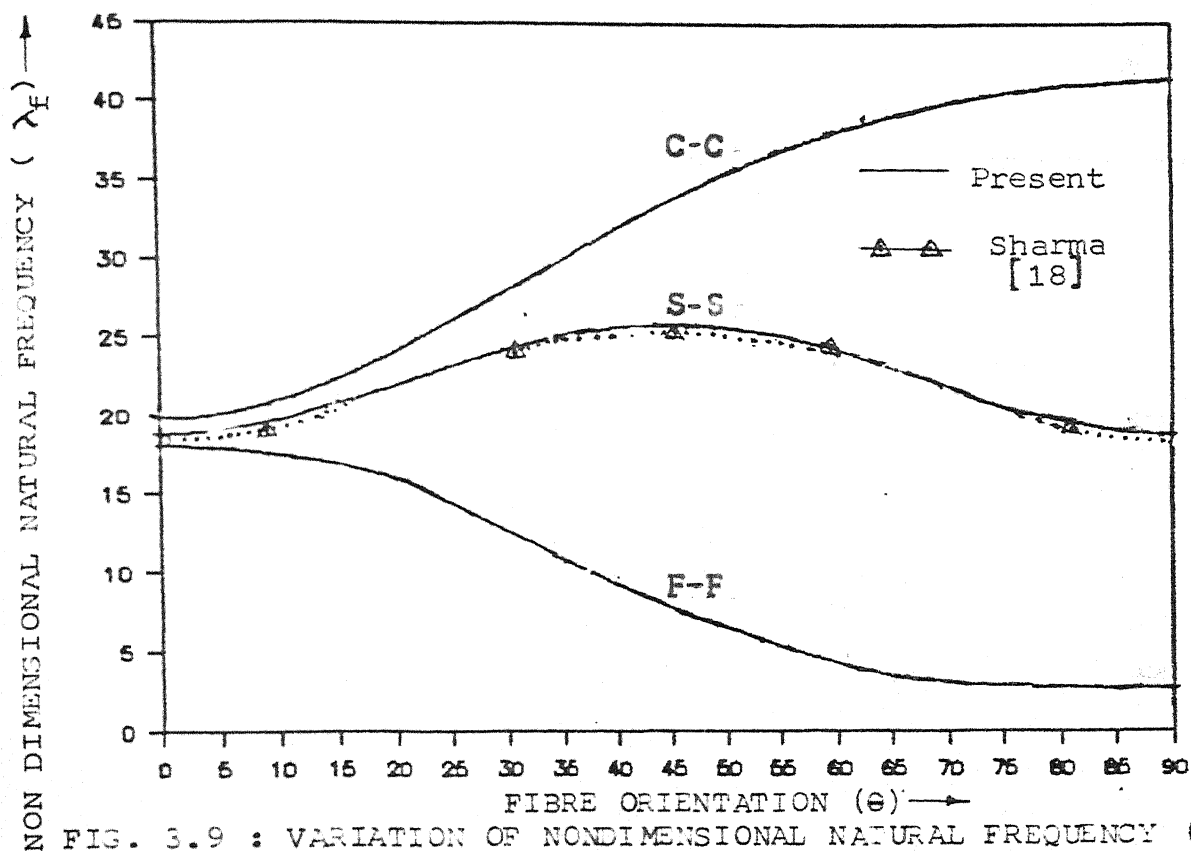


FIG. 3.9 : VARIATION OF NONDIMENSIONAL NATURAL FREQUENCY (λ_F) WITH FIBRE ORIENTATION (θ). (AR = 1.0)

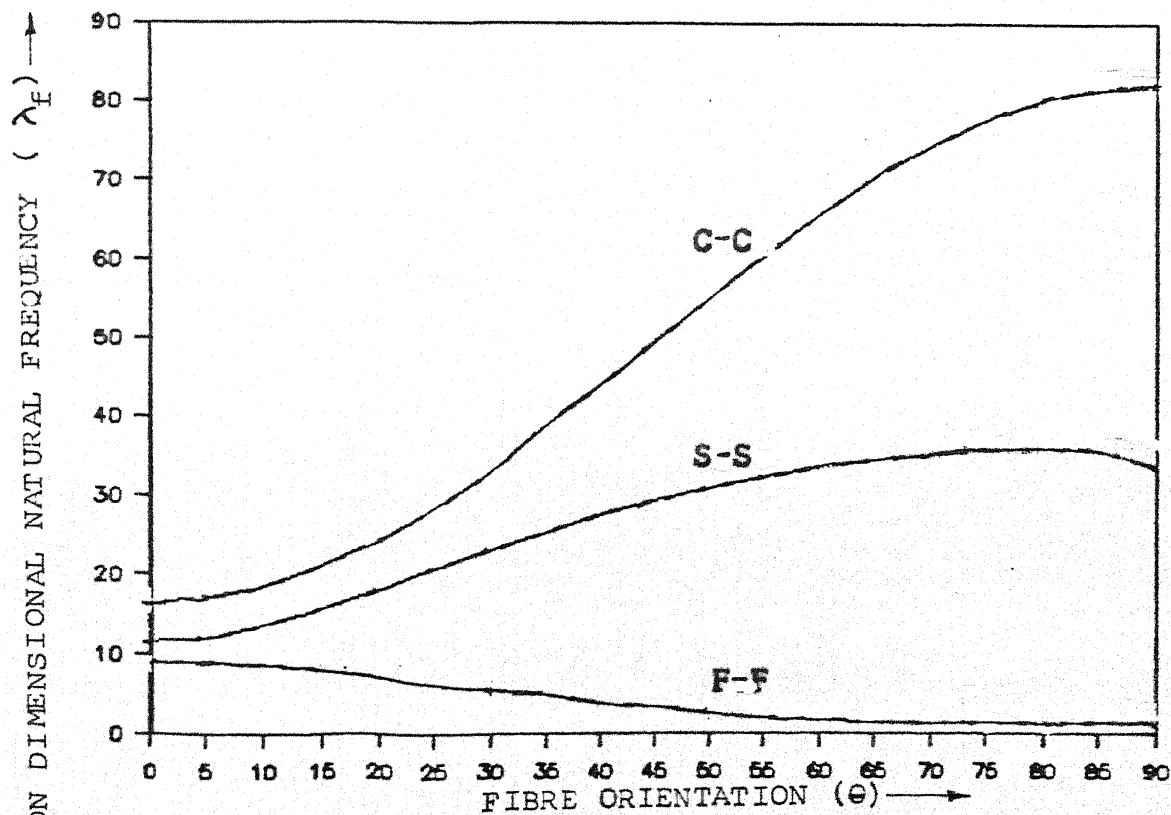


FIG.3.10. VARIATION OF NONDIMENSIONAL NATURAL FREQUENCY (λ_F)

Table 3.1 : Effect of Aspect ratios in Decoupled Laminate

AR=0.5		AR=1.0		AR=1.5		AR=2.0	
m=1	m=2	m=1	m=2	m=1	m=2	m=1	m=2
186.65	350.74	80.02	127.73	88.83	129.98	121.04	88.60
146.72	600.20	<u>79.36</u>	142.39	88.03	138.51	111.04	79.50
131.97	352.46		132.42	87.02	132.93	11.00	<u>79.16</u>
135.88	489.12		135.20	<u>87.75</u>	134.50		101.28
130.31	354.03		133.39		133.47		100.48
	356.66		133.91				
<u>130.90</u>							

Table 3.2 : Effect of starting functions, mesh size and convergence criteria

λ_{d1}	λ_{d2}	λ_{d3}	λ_{d4}
89.13	168.23	89.12	89.13
88.03	84.12	88.04	88.03
87.02	88.26	87.01	87.02
87.75	97.98	87.75	87.75
	87.75		87.71

CHAPTER - IV

ANALYSIS OF COUPLED LAMINATES

In this chapter a study has been made to analyse coupled antisymmetric angle ply laminates. Using successive iteration technique. A detailed investigation has been carried out with various computational models for uniaxial buckling problems with x edges simply supported and y edges clamped.

4.1 GOVERNING EQUATIONS

The eqn. (2.15) can be rearranged for uniaxial buckling problem as,

$$w^{IV} = c_1 w'' + c_2 w + c_3 v + c_4 u' + c_5 v'' + c_6 u'' \quad (4.1a)$$

$$v'' = c_7 w'' + c_8 w + c_9 v + c_{10} u' \quad (4.1b)$$

$$u'' = c_{11} w'' + c_{12} w' + c_{13} v' + c_{14} u \quad (4.1c)$$

where

$$c_1 = -\frac{e_2}{e_1}; \quad c_2 = z_1 - z_2 \lambda; \quad z_1 = -\frac{D_{11} \alpha^4}{e_1};$$

$$z_2 = -\frac{\alpha^2 p^2}{e_1}; \quad c_3 = -\frac{e_5}{e_1};$$

$$c_4 = -\frac{e_7}{e_1}; \quad c_5 = -\frac{e_4}{e_1}; \quad c_6 = -\frac{e_6}{e_1};$$

$$c_7 = -\frac{e_8}{e_{10}}; \quad e_8 = -\frac{e_9}{e_{10}};$$

$$\begin{aligned}
c_9 &= -\frac{e_{11}}{e_{10}}; \quad c_{10} = -\frac{e_{12}}{e_{10}}; \quad c_{11} = -\frac{e_{13}}{e_{16}}; \\
c_{12} &= -\frac{e_{14}}{e_{16}}; \quad c_{13} = -\frac{e_{15}}{e_{16}}; \quad c_{14} = -\frac{e_{17}}{e_{16}} \quad (4.1d)
\end{aligned}$$

It may be rementioned that

$e_1, e_2, e_3, \dots, e_{16}$ are defined in eqn. (2.8d)

with
$$K = \frac{\bar{N}_y}{\bar{N}_x} = 0$$

Prime denotes the differentiation with respect to η .

Integrating eqn. (4.1a) successively one gets,

$$w''' = c_1 w' + c_2 \int_0^\eta w \, d\eta + c_3 \int_0^\eta v \, d\eta + c_4 u + c_5 v' + c_6 u'' + k_1 \quad (4.2a)$$

$$\begin{aligned}
w'' &= c_1 w + c_2 \int_0^\eta \int_0^\eta w \, d\eta^2 + c_3 \int_0^\eta \int_0^\eta v \, d\eta^2 + c_4 \int_0^\eta u \, d\eta + c_5 v \\
&\quad + c_6 u' + k_1 \eta + k_2 \quad (4.2b)
\end{aligned}$$

$$\begin{aligned}
w' &= c_1 \int_0^\eta w \, d\eta + c_2 \int_0^\eta \int_0^\eta \int_0^\eta w \, d\eta^3 + c_3 \int_0^\eta \int_0^\eta \int_0^\eta v \, d\eta^3 \\
&\quad + c_4 \int_0^\eta \int_0^\eta u \, d\eta^2 + c_5 \int_0^\eta v \, d\eta + c_6 u + \frac{k_1 \eta^2}{2} \\
&\quad + k_2 \eta + k_3 \quad (4.2c)
\end{aligned}$$

$$\begin{aligned}
w &= c_1 \int_0^\eta \int_0^\eta w \, d\eta^2 + c_2 \int_0^\eta \int_0^\eta \int_0^\eta \int_0^\eta w \, d\eta^4 + c_3 \int_0^\eta \int_0^\eta \int_0^\eta \int_0^\eta v \, d\eta^4 \\
&\quad + c_4 \int_0^\eta \int_0^\eta \int_0^\eta u \, d\eta^3 + c_5 \int_0^\eta \int_0^\eta v \, d\eta^2 + c_6 \int_0^\eta u \, d\eta + \frac{k_1 \eta^3}{6} \\
&\quad + k_2 \frac{\eta^2}{2} + k_3 \eta + k_4 \quad (4.2d)
\end{aligned}$$

Integration of eqn. (4.1b) and eqn. (4.1c) yields

$$v' = c_7 w' + c_8 \int_0^\eta w d\eta + c_9 \int_0^\eta v d\eta + c_{10} u + k_5 \quad (4.2e)$$

$$v = c_7 w + c_8 \int_0^\eta \int_0^\eta w d\eta^2 + c_9 \int_0^\eta \int_0^\eta v d\eta^2 + c_{10} \int_0^\eta u d\eta + k_5 \eta + k_6 \quad (4.2f)$$

$$u' = c_{11} w'' + c_{12} w' + c_{13} v' + c_{14} \int_0^\eta u d\eta + k_7 \quad (4.2g)$$

$$u = c_{11} w' + c_{12} \int_0^\eta w d\eta + c_{13} \int_0^\eta v d\eta + c_{14} \int_0^\eta \int_0^\eta u d\eta^2 + k_7 \eta + k_8 \quad (4.2h)$$

The constants of integrations $k_1, k_2, k_3, k_4, k_5, k_6, k_7, k_8$ are to be determined from the boundary conditions.

4.2 RAYLEIGH'S QUOTIENT

Using eqn. (2.18) and eqn. (2.20a), the Rayleigh's quotient can be written as

$$\lambda = (H_1 + H_2 + H_3 + H_4 + H_5 + H_6 + H_7 + H_8 + H_9 + H_{10})/H_{11} \quad (4.3a)$$

where

$$H_1 = \bar{A}_{11} \alpha^2 V^2 \int_0^1 (u)^2 d\eta \quad (4.3b)$$

$$H_2 = 2\bar{A}_{12} p r^2 \alpha \int_0^1 (u v') d\eta \quad (4.3c)$$

$$H_3 = \bar{A}_{22} p^2 r^2 \int_0^1 (v')^2 d\eta \quad (4.3d)$$

$$H_4 = \bar{A}_{66} r^2 \int_0^1 (p^2 (u')^2 - 2/p(u'v) + v^2 \alpha^2) d\eta \quad (4.3e)$$

$$H_5 = 2\bar{B}_{16} r \alpha^2 \int_0^1 ((u'w) p - (vw)\alpha - 2(uv')p) d\eta \quad (4.3f)$$

$$H_6 = 2\bar{B}_{26} r p^2 \int_0^1 (-(u'w'') p + (vw'')\alpha - 2(v'w')\alpha) d\eta \quad (4.3g)$$

$$H_7 = \bar{D}_{11} \alpha^4 \int_0^1 w^2 d\eta \quad (4.3h)$$

$$H_8 = -2\bar{D}_{12} p^2 \alpha^2 \int_0^1 (ww'') d\eta \quad (4.3i)$$

$$H_9 = \bar{D}_{22} \int_0^1 (w'')^2 d\eta \quad (4.3j)$$

$$H_{10} = 4\bar{D}_{66} \int_0^1 (w')^2 d\eta \quad (4.3k)$$

$$H_{11} = p^2 \alpha^2 \int_0^1 w^2 d\eta \quad (4.3l)$$

4.3 BOUNDARY CONDITION

Using the relations (2.14a) to (2.14c) in eqn.(2.13c), boundary conditions for clamped y edges are obtained as

$$\begin{aligned} u(0) &= v(0) = w(0) = w'(0) = 0 \\ u(1) &= v(1) = w(1) = w'(1) = 0 \end{aligned} \quad (4.4)$$

The constants of integration can be obtained using (4.4) in (4.2b) to (4.2h). Defining the definite integrals as,

$$\begin{aligned}
 r_1 = & c_1 \int_0^1 \int_0^\eta w d\eta^2 + c_2 \int_0^1 \int_0^\eta \int_0^\eta w d\eta^3 + c_3 \int_0^1 \int_0^\eta \int_0^\eta v d\eta^3 \\
 & + c_4 \int_0^1 \int_0^\eta u d\eta^2 + c_5 \int_0^1 v d\eta + c_6 u(1)
 \end{aligned} \quad (4.5a)$$

$$\begin{aligned}
 r_2 = & c_1 \int_0^1 \int_0^\eta \int_0^\eta w d\eta^3 + c_2 \int_0^1 \int_0^\eta \int_0^\eta \int_0^\eta w d\eta^4 \\
 & + c_3 \int_0^1 \int_0^\eta \int_0^\eta \int_0^\eta v d\eta^4 + c_4 \int_0^1 \int_0^\eta \int_0^\eta u d\eta^3 \\
 & + c_5 \int_0^1 \int_0^\eta v d\eta^2 + c_6 \int_0^1 u d\eta
 \end{aligned} \quad (4.5b)$$

$$r_3 = c_7 \int_0^1 w d\eta + c_8 \int_0^1 \int_0^\eta w d\eta^2 + c_9 \int_0^1 \int_0^\eta v d\eta^2 + c_{10} \int_0^1 u d\eta \quad (4.5c)$$

$$r_4 = c_{11} w'(1) + c_{12} \int_0^1 w d\eta + c_{13} \int_0^1 v d\eta + c_{14} \int_0^1 \int_0^\eta u d\eta^2 \quad (4.5d)$$

Constants of integrations are

$$\begin{aligned}
 k_1 &= 12r_2 - 6r_1; \quad k_2 = 2r_1 - 6r_2; \quad k_3 = 0; \quad k_4 = 0; \quad k_5 = -r_3 \\
 k_6 &= 0; \quad k_7 = -r_4; \quad k_8 = 0
 \end{aligned} \quad (4.5e)$$

4.4 GENERAL STEPS IN SUCCESSIVE ITERATION TECHNIQUE

1. For the given fibre and matrix properties E_1 , E_2 , G_{12} and γ_{12} generate $[Q]$ and $[\bar{Q}]$ matrices using eqn. (2.4) and eqn. (2.5) respectively.

2. For the chosen θ and thicknesses of the laminate, compute the coefficients of the stiffness matrices A_{ij} , B_{ij} and D_{ij} from eqns.(2.8).
3. For the specified aspect ratio (p), length to thickness ratio (r) and given mode number, calculate the constants c_1 , z_1 , z_2 , c_3 , c_4 , c_5 , c_6 , c_7 , c_8 , c_{10} , c_{11} , c_{12} from eqn. (4.1d).
4. Select some initial functions w, v, u (say $w(\eta) = v(\eta) = u(\eta) = 1$) which may or may not satisfy the boundary conditions and an arbitrary eigen value (say $\lambda = 10$).
5. Find the value of c_2 from eqn. (4.1d).
6. The constants of integration k_3 , k_4 , k_6 , k_8 are zero. Evaluate the constants k_1 , k_2 , k_5 and k_7 from the eqns. (4.6a) to (4.6e).
7. Using the same already obtained or initialised functions w_n'' , w_n' , w_n , u_n' , v_n , u_n' and u_n , independently evaluate w_{n+1}'' , w_{n+1}' , w_{n+1} , v_{n+1}' , v_{n+1} , u_{n+1}' and u_{n+1} from eqns. (4.2b) to (4.2h). The suffix n denotes the iteration number.
8. Normalize the functions w_{n+1}'' , w_{n+1}' , w_{n+1} , v_{n+1}' , v_{n+1} , u_{n+1}' , u_{n+1} using a scalar factor (say w_{\max}).
9. Determine the eigen value λ from the eqn. (4.3a).
10. Return the control to step 5 and terminate the iteration, when $|(\lambda_{n+1} - \lambda_n)/\lambda_n| \leq \epsilon$, a small number (say $\epsilon = 0.001$).

11. For various values of mode numbers, find the eigen values λ_{n+1} . The minimum eigen value out of these eigen values is the buckling load.

4.4.1 NUMERICAL STUDY

Numerical computation was carried out on GFRP six layered regular (equal thicknesses) laminate, with same material properties as mentioned in Chapter III. Table 4.1 shows the eigen values obtained in the iteration process for $m = 1$ and 2 and buckling loads for various fibre orientations θ . A mesh size of 0.01 was selected for quadrature using trapezoidal rule. Following observations can be made from table 4.1.

1. For $\theta = 20$ and $m = 1$, the iteration converged at an eigen value 97.91 . For $m = 2$, it converged at 171.60 . The buckling load 97.91 has an error of about 78% compared to Sharma's [18] 55 .
2. For $\theta = 30$ and $m = 1$, the iteration converged at an eigen value 110.78 . For $m = 2$ it converged at 152.72 . The buckling load 110.78 has an error of about 73% compared to Sharma's [18] 64 .
3. For $\theta = 45^\circ$ and $m = 1$, the iteration converged at an eigen value 133.72 . For $m = 2$ it converged at 142.63 . The buckling load 133.72 has an error of about 39.53% compared to Sharma's [18] 96.

4. Load increases as θ increases for 45° . This general trend agrees with the correct result
5. As the error involved is very large a detailed investigation in the case of $\theta = 20^\circ$ was carried out.

Though convergence in eigen value was obtained in all the above cases tested, the value of the buckling loads are not correct. Various tests had to be made to check this behaviour. i) A test could be made to see the convergence behaviour of the iteration process, by using different starting functions say $w(\eta) = \sin^2 \pi \eta$; $u(\eta) = \sin \pi \eta$; $v(\eta) = \sin \pi \eta$ which satisfy the boundary conditions; ii) A test could be made to see the possibility of round off errors that may occur in the iteration process, by using double precision facility throughout the program; iii) A test could be made to see the influence of starting eigen value, by using the eigen value λ obtained from Rayleigh's quotient eqns. (4.3a) to (4.3l) for the initial functions $w(\eta) = v(\eta) = u(\eta) =$ as starting value rather than previously assigned ($\lambda = 10$) value; iv) A test could be made to see the influence of the mesh size, by selecting mesh interval, say 0.001 instead of 0.01 in the quadrature using trapezoidal rule.

Table 4.2 gives the eigen values for the following cases:

- i) Convergence of iteration was achieved even when different starting function were used. The converged

- ei eigen value (λ_f) for the starting functions
 $w(\eta) = v(\eta) = u(\eta) = 1$ was 97.91 and for
 $w = \sin^2 \pi \eta$; $v = \sin \pi \eta$; $u = \sin \pi \eta$ the
 converged eigen value (λ_2) was 97.79, though
 the initially obtained eigen values are differ-
 ent from the previous case. This indicates that
 the iteration process is moving smoothly and is
 independent of starting functions.
- ii) Computations in double precision do not affect
 the results. The large discrepancy in results
 does not seem to be occurring due to round off
 errors. (λ_3) values converges to 97.91.
- iii) For a starting eigen value $\lambda = 50$, the obtained,
 converged eigen value was 97.91 and for the
 second case using the starting eigen value got from
 the Rayleigh's quotient equation was (λ_4) 97.58.
 This indicates that the iteration process is
 independent of starting eigen value and it is trying
 to achieve the same convergence even though the
 initially obtained eigen values in both the cases
 are different.
- iv) The use of mesh size 0.001 instead of 0.01 gives
 the same iterated eigen values and the converged
 eigen value (λ_5) 97.91.

It may be presumed that evaluating the functions w''_{n+1} , w'_{n+1} , w_{n+1} , v'_{n+1} , v_{n+1} , u'_{n+1} and u_{n+1} independently from eqns. (4.2b) to (4.2h) using the already obtained functions w''_n , w'_n , w_n , v'_n , v_n , u'_n and u_n might have led to this incorrectness of the convergence. By using, the improved functions (say u_{n+1} , v_{n+1}) in addition to the already obtained functions (say w_n), in the evaluation of functions (say w_{n+1}) from eqns. (4.2b) to (4.2h) one may expect better result. Various combinations are possible in the simultaneous iteration of functions and various models could be studied.

4.5 ITERATION SEQUENCES IN MODELS

The previous iteration scheme is denoted as model 1. In all the other models to be studied, only the steps 5 to 9 of Model 1 had to be replaced.

4.5.1 MODEL 2

- i) Choose the initial functions $w(\eta) = v(\eta) = u(\eta) = 1$ and an initial eigen value $\lambda = 10$.
- ii) Evaluate u'_{n+1} and u_{n+1} from eqns. (4.2g) and (4.2h), using the functions w''_n , w'_n , w_n , v_n and u_n .
- iii) Evaluate v'_{n+1} and v_{n+1} from eqns. (4.2e) and (4.2f), using the functions w'_n , w_n , v_n and u_{n+1} .
- iv) Evaluate w''_{n+1} , w'_{n+1} , w_{n+1} from eqns. (4.2b), (4.2c) and (4.2d), using the functions u'_{n+1} , u_{n+1} , v_{n+1} and w_n .

- v) Normalise the function w''_{n+1} , w'_{n+1} , w_{n+1} , v'_{n+1} , v_{n+1} , u'_{n+1} and u_{n+1} using the maximum value of w_{n+1} .
- vi) Find the eigen value λ from eqn. (4.3a).

4.5.2 MODEL 3

- i) Choose the initial functions $u(\eta) = v(\eta) = u(\eta) = 1$ and an initial eigen value $\lambda = 10$.
- ii) Evaluate u''_{n+1} and u'_{n+1} using the functions w''_n , w'_n , w_n , v_n and u_n .
- iii) Evaluate v'_{n+1} and v_{n+1} using the functions w'_n , w_n , v_n and u_{n+1} .
- iv) Normalise the functions w''_n , w'_n , w_n , v'_{n+1} , v_{n+1} , u'_{n+1} and u_{n+1} using the maximum value of w_n .
- v) Find λ from eqn. (4.3a).
- vi) Evaluate w''_{n+1} , w'_{n+1} , w_{n+1} using the functions u'_{n+1} , u_{n+1} , v_{n+1} and w_n .

4.5.3 MODEL 4

- i) Choose the initial functions $w(\eta) = v(\eta) = u(\eta) = 1$ and an initial eigen value $\lambda = 10$.
- ii) Evaluate w''_{n+1} , w'_{n+1} and w_{n+1} using the functions u'_n , u_n , v_n and w_n .
- iii) Evaluate v'_{n+1} and v_{n+1} using the functions w'_{n+1} , w_{n+1} , v_n and u_n .

- iv) Evaluate u'_{n+1} and u_{n+1} from eqns. (4.2g) and (4.2h), using the functions w''_{n+1} , w'_{n+1} , w_{n+1} , v_{n+1} and u_n .
- v) Normalise the functions w''_{n+1} , w'_{n+1} , w_{n+1} , v'_{n+1} , v_n , u'_{n+1} and u_n using the maximum value of w_{n+1} .
- vi) Find the eigen value λ .

4.5.4 MODEL 5

- i) Choose the initial functions $w(\eta) = v(\eta) = u(\eta) = 1$ and an initial eigen value $\lambda = 10$.
- ii) Evaluate w''_{n+1} , w'_{n+1} , w_{n+1} using the functions u'_n , u_n , v_n and w_n .
- iii) Evaluate u'_{n+1} and u_{n+1} using the functions w''_{n+1} , w'_{n+1} , w_{n+1} , v_n and u_n .
- iv) Evaluate v'_{n+1} and v_{n+1} using the functions w'_{n+1} , w_{n+1} , v_n and u_{n+1} .
- v) Normalise w''_{n+1} , w'_{n+1} , w_{n+1} , v'_{n+1} , v_{n+1} , u'_{n+1} and u_{n+1} using maximum value of w_{n+1} .
- vi) Find the eigen value λ from Rayleigh's quotient eqn. (4.3a).

4.5.5 MODEL 6

- i) Choose the initial functions $w(\eta) = v(\eta) = u(\eta) = 1$.
- ii) Evaluate v'_{n+1} and v_{n+1} from eqns. (4.2e) and (4.2f), using the functions w'_n , w_n , v_n , u_n .
- iii) Normalise the functions w''_n , w'_n , w_n , v'_{n+1} , v_{n+1} , u'_n using the maximum value of w_n .

- iv) Find the eigen value λ .
- v) Evaluate w''_{n+1} , w'_{n+1} , w_{n+1} using the functions u'_n , u_n , v_{n+1} and w_n .
- vi) Evaluate u'_{n+1} , u_{n+1} using the functions w''_{n+1} , w'_{n+1} , w_{n+1} , v_{n+1} and u_n .

4.6 NUMERICAL STUDY IN MODELS

The same GFRP six layered regular 20° angle ply laminate was taken for numerical study in various models. Table 4.3 shows the eigen values obtained in the iteration process for the models. The starting function was selected as $w(\eta) = v(\eta) = u(\eta) = 1$. A mesh size of 0.01 was used in the quadrature using trapezoidal rule.

Following observations can be made from a study of the table:

- i) In model 2, the iterated eigen values oscillate between 64 to 78 in the initial five iteration and finally it converged smoothly at a value of 81.39.
- ii) In model 3, the iterated eigen values oscillated between 64 to 77 in the first five iterations and finally it converged at a value of 80.88.
- iii) In model 4, the iterated eigen values oscillated between 69 to 86 in the first five iterations and finally converged at 79.58 after another three iterations.

- iv) In model 5, the iterated eigen values oscillated between 70 to 84 in the first five iteratives and converged at 81.07 after another nine iterations.
- v) In model 6, the iterated eigen values converged in five iterations to a value of 79.24.
- vi) Compared to model 1, all the above models are converging closely around 80. These models are better than model 1, which converged at a value around 98. As these results differ by about 50% with the correct results, model 5 was further investigated.

4.7 DETAILED NUMERICAL ANALYSIS IN MODEL 5

A detailed study could be made to analyze the eigen values in model 5 iterations scheme, by varying the number of layers in GFRP 20° angle ply regular laminate. Table 4.4 shows the eigen values obtained in the model 5 iterations process for varied number of layers from 2 to 50.

- i) In 2 layered laminate, the iteration converged at 74.25. Sharma [18] obtained the buckling load as 26. The error is about 185%.
- ii) For 4 layered laminate, the iteration converged at 74.74. Sharma [18] obtained the buckling load as 48. The error is about 55%.

- iii) For 6 layered laminate, the iteration converged at 81.07. Sharma 18 obtained the buckling load as 55. The error is about 47%.
- iv) For 20 layered laminate the iteration converged at 85.27. Sharma 18 obtained the buckling load for infinity layers as 58. The error is about 46%.
- v) For 50 layered laminate the iteration converged at 86.01.
- vi) As the number of layers are increased, the converged eigen value also increases gradually. This behaviour is logically true in laminate analysis. The coupling coefficients B_{16} and B_{26} approach zero as the number of layers are increased and the laminate behave as decoupled laminate. The error in percentage is reduced as the number of layers are increased in this model scheme. This indicates that the presence of B_{16} and B_{26} terms has influence in obtaining the buckling load.

In thin classical plate theory, the effect of thickness to length ratio (r) is not felt. But the governing equations used in the present investigation appear to be dependent upon r . A study of the dependence of on r is presented in Table 4.5.

Table 4.5 shows the (i) eigen values obtained for $r = 1$ case in 20° six ply regular GFRP laminate with starting functions $w(\eta) = v(\eta) = u(\eta) = 1$, (ii) $r = 1$ case with starting functions $w(\eta) = v(\eta) = w(\eta) = 1$ and (iii) $r = 20$ case with starting functions $w(\eta) = \sin^2 \pi \eta$; $v(\eta) = \sin \pi \eta$; $u(\eta) = \sin \pi \eta$. The following observations could be made:

- i) The value of r is not at all influencing the convergence of the iteration process. For $r = 1$ and 20 and for different starting functions the eigen value converged to same 81.07.

Table 4.6 shows the values of u , v and w displacements at various discrete points and the constants of integration k_1 , k_2 , k_3 and k_4 for the final two stages of iteration process in six layered regular GFRP 20° laminate.

Though the w values converged at the final two stages of iteration, the u and v values did not converge. The constants of integration k_1 , k_2 , k_5 and k_7 were also not converging because of the non-convergence of u , v . The incorrect buckling load might have obtained due to this behaviour.

Table 4.7 shows the values of the particular integral terms $H_1, H_2, H_3, H_4, \dots, H_{11}$ appearing in the Rayleigh's quotient eqn. (4.3a) for the final two stages of iteration in six layered GFRP 20° laminate. Convergence in each terms $H_1, H_2, H_3, H_4, H_5, H_6, H_7, H_8, H_9, H_{10}$ and H_{11} are achieved for final successive stages of iteration as observed in

table 4.7. This indicates that convergence occurs in each individual particular integral terms of the Rayleigh's quotient expression in addition to the eigen value .

The solution technique, appears to give the solution of the eqns. (4.1a) to (4.1c). However, the iteration converges to incorrect results. Detailed investigation reveals the convergence on the eigen value, but the mode shape, specially inplane displacements u and v , donot converge properly. It is difficult to pinpoint the reasons. Probably this is due to inherent limitation of the method. One of the reasons could be seeking of the convergence on three variables u , v and w through iteration.

It is possible to reduce the present set of governing equations into a set of two fourth order ordinary differential equation in v and w , by eliminating the variable u . The solution then boils down to solution involving only two unknown dependent variables. This approach is presented in the next section.

4.8 SOLUTION USING TWO VARIABLES v and w

The governing equations (4.1a) to (4.1c) are rewritten here for clarity sake.

$$w^{IV} = c_1 w'' + c_2 w + c_3 v + c_4 u' + c_5 v'' + c_6 u'' \quad (4.1a)$$

$$v'' = c_7 w'' + c_8 w + c_9 v + c_{10} u' \quad (4.1b)$$

$$u'' = c_{11} w'' + c_{12} w' + c_{13} v' + c_{14} u \quad (4.1c)$$

From eqn. (4.1b), one gets,

$$u' = d_1 v'' + d_2 v' + d_3 w'' + d_4 w \quad (4.6)$$

Elimination of u'' from eqns. (4.1c) and (4.6) gives

$$u = f_1 v''' + f_2 v' + f_3 w''' + f_4 w' \quad (4.7)$$

$$u' = f_1 v^{IV} + f_2 v'' + f_3 w^{IV} + f_4 w'' \quad (4.8)$$

Substituting u' from eqn. (4.4) into eqn. (4.2), one gets

$$v^{IV} = g_1 v'' + g_2 v' + g_3 w^{IV} + g_4 w''' + g_5 w'' + g_6 w \quad (4.9)$$

It may be noted that in the above equation, following constants have been defined:

$$\begin{aligned} d_1 &= \frac{1}{c_{10}} ; d_2 = -\frac{c_9}{c_{10}} ; d_3 = -\frac{c_7}{c_{10}} ; d_4 = -\frac{c_8}{c_{10}} \\ f_1 &= \frac{d_1}{c_{14}} ; f_2 = \frac{(d_2 - c_{13})}{c_{14}} ; f_3 = \frac{(d_3 - c_{11})}{c_{14}} ; f_4 = \frac{(d_4 - c_{12})}{c_{14}} \end{aligned} \quad (4.10)$$

$$\begin{aligned} g_1 &= \frac{(d_1 - f_2)}{f_1} ; g_2 = \frac{d_2}{f_1} ; g_3 = -\frac{f_3}{f_1} ; g_4 = \frac{d_3}{f_1} ; g_5 = -\frac{f_4}{f_1} ; \\ g_6 &= \frac{d_4}{f_1} . \end{aligned}$$

Integrating eqn. (4.9) successively, one obtains

$$v''' = g_1 v' + g_2 \int_0^\eta v \, d\eta + g_3 w''' + g_4 w'' + g_5 w' + g_6 \int_0^\eta w \, d\eta + k_9 \quad (4.11)$$

$$v'' = g_1 v + g_2 \int_0^\eta \int_0^\eta v d\eta^2 + g_3 w'' + g_4 w' + g_5 w + g_6 \int_0^\eta \int_0^\eta w d\eta \\ + k_9 \eta + k_{10} \quad (4.12)$$

$$v' = g_1 \int_0^\eta v d\eta + g_2 \int_0^\eta \int_0^\eta \int_0^\eta v d\eta^3 + g_3 w' + g_4 w + g_5 \int_0^\eta w d\eta \\ + g_6 \int_0^\eta \int_0^\eta \int_0^\eta w d\eta^3 + k_9 \frac{\eta^2}{2} + k_{10} \eta + k_{11} \quad (4.13)$$

$$v = g_1 \int_0^\eta \int_0^\eta v d\eta^2 + g_2 \int_0^\eta \int_0^\eta \int_0^\eta v d\eta^4 + g_3 w + g_4 \int_0^\eta w d\eta \\ + g_5 \int_0^\eta \int_0^\eta w d\eta^2 + g_6 \int_0^\eta \int_0^\eta \int_0^\eta \int_0^\eta w d\eta^4 + k_9 \frac{\eta^3}{6} \\ + k_{10} \frac{\eta^2}{2} + k_{11} \eta \quad (4.14)$$

Using the boundary conditions ($v(1) = u(0) = u(1) = 0$), constants k_9 , k_{10} , k_{11} can be evaluated as a solution of a set of three linear algebraic equations. Omitting the details the constants can be evaluated from the relations.

$$k_9 = \frac{s_9}{s_{10}}, \quad k_{10} = s_6 \cdot k_9 + s_7, \quad k_{11} = s_2 + s_3 k_9 \quad (4.15)$$

where the following constants are required to determine k_9 , k_{10} and k_{11} :

$$s_1 = g_1 v'(0) + g_3 w'''(0) + g_4 w''(0) \quad (4.16)$$

$$s_2 = - \frac{(f_1 s_1 + f_3 w'''(0))}{f_2}, \quad s_3 = - \frac{f_1}{f_2} \quad (4.17)$$

$$s_4 = g_1 v'(1) + g_2 \int_0^1 v d\eta + g_3 w'''(1) + g_4 w''(1) + g_6 \int_0^1 w d\eta \quad (4.18)$$

$$s_5 = g_1 \int_0^1 v d\eta + g_2 \int_0^1 \int_0^\eta \int_0^\eta v d\eta^3 + g_5 \int_0^1 w d\eta + g_6 \int_0^1 \int_0^\eta \int_0^\eta w d\eta^3 \quad (4.19)$$

$$s_6 = - \frac{(f_1 + f_2 (s_3 + 0.5))}{f_2} ;$$

$$s_7 = - \frac{(f_1 s_4 + f_2 (s_5 + s_2) + f_3 w''(1))}{f_2} \quad (4.20)$$

$$s_8 = g_1 \int_0^1 \int_0^\eta v d\eta^2 + g_2 \int_0^1 \int_0^\eta \int_0^\eta \int_0^\eta v d\eta^4 + g_4 \int_0^1 w d\eta + g_5 \int_0^1 \int_0^\eta w d\eta^2 + g_6 \int_0^1 \int_0^\eta \int_0^\eta \int_0^\eta w d\eta^4 \quad (4.21)$$

$$s_9 = -(s_8 + s_2 + \frac{s_7}{2}) ; \quad s_{10} = s_3 + \frac{s_6}{2} + \frac{1}{6} \quad (4.22)$$

It is quite evident that successive integration on eqn. (4.9) can be carried out to determine v .

We now need to eliminate u from the eqn. (4.1a) for w . Using eqns. (4.1b) and (4.1c), w equation can be rewritten as

$$w^{IV} = c_{15} w'' + c_{16} w + c_{17} v + c_{18} u' \quad (4.23)$$

where

$$u' = d_1 v'' + d_2 v' + d_3 w'' + d_4 w \quad (4.7)$$

$$u = f_1 v''' + f_2 v'' + f_3 w''' + f_4 w' \quad (4.8)$$

and constants

$$\begin{aligned}
c_{15} &= - \frac{(e_6 c_5 c_{11} + e_4 c_5 + e_6 c_{10} + e_2)}{(e_1 + e_6 c_9)} , \\
c_{16} &= z_7 - z_8 \lambda ; z_7 = - \frac{(c_6 e_4 + c_6 e_6 c_{11} + \bar{D}_{11} \alpha^4)}{(e_1 + e_6 c_9)} , \\
z_8 &= - \frac{(\alpha^2 p^2)}{(e_1 + e_6 c_9)} ; c_7 = - \frac{(e_5 + c_7 e_4 + c_7 e_6 c_{11})}{(e_1 + e_6 c_9)} , \\
c_{18} &= - \frac{(e_7 + e_6 c_{12} + e_4 c_8 + e_6 c_8 c_{11})}{(e_1 + e_6 c_9)} \quad (4.24)
\end{aligned}$$

The present problem, thus, boils down to the solution of fourth order eqns. (4.9) and (4.23) in v and w . For known v and w , u' and u which are required to evaluate are determined from eqns. (4.7) and (4.8) respectively.

4.9 NUMERICAL STUDY WITH TWO VARIABLES

Solution was obtained for the laminate used in section 4.4.1 for $\theta = 20^\circ$. Two models for iteration were used.

4.9.1 MODEL 1

Iteration follows similar procedure as used in the case of three variables. A very brief outline is given below.

1. Choose the initial functions and λ as

$$\begin{aligned}
v &= \eta(\eta - 1) \\
w &= \sin^2 \pi \eta \\
\lambda &= 50
\end{aligned}$$

2. Determine v and then u from eqn. (4.7).
3. Using above computed v , u determine w and calculate λ .
4. Determine u and u' .
5. Normalise u , v and w with respect to w_{\max} . Go back to step 2 and continue iteration till converges.

Numerical results obtained for $m = 1$ and 2 are presented in Table 4.8 which gives λ associated with each iteration cycle. For $m = 1$, iteration does not converge. Eigen value finally appears to oscillate between 59.2 and 190 (approx.) . However for $m = 2$ convergence occurs in 3 iterations. It was further observed that the mode shapes is displacement functions u , v and w converged accurately.

4.9.2 MODEL 2

In the previous case v obtained after iteration was used in computing w . In this case w equation is integrated without using previously calculated v i.e. integration of the two equations is carried out independently. For $m = 1$ λ associated with first few iterations is presented in Table 4.8. Oscillations observed in model 1 were also seen in this case.

4.10 GENERAL OBSERVATIONS

A relatively detailed investigation was made. The results obtained are not presented here. However, following general comments based on the study can be made.

1. The value of $\lambda = 56.2$ i.e. Model 2 is the exact result. Value $\lambda = 59.2$ is fairly close to this value. The iteration thus appears to oscillate between a correct and highly incorrect value. Correct value was obtained within first few iterations. One tends to believe that the method yields reasonably correct results in 4 to 5 iterations. So using model 2, a study was made for different values of θ . Results do not substantiate the conclusions reached for $\theta = 20^\circ$.
2. For $m = 2$, precise convergence occurs for $\theta = 20^\circ$. It is a highly perplexing behaviour as no other change, except in the value of m , has been made. Probably the solution process is very sensitive to the values of the coefficients of the derivatives on the right hand side of the equations (4.9) and (4.23). Oscillations were observed for $m = 2$ when θ was varied.
3. It appears that successive iteration in such problems may lead to correct result. It has, however, failed to give the desired solution in the present study. Even if the method may work in some cases, its reliability when the number of dependent variables is more than 1 appears to be doubtful. The method, therefore, should be attempted when the dependent

variable is only 1.

4. Logically, the method seems to be acceptable. Investigation attempted in the present study are unable to pinpoint the reasons behind the failures of the method.

Table 4.1 : Effect of fibre orientations

$\lambda (\theta = 20^\circ)$			$\lambda (\theta = 30^\circ)$			$\lambda (\theta = 45^\circ)$		
m=1	m=2	m=1	m=2	m=1	m=2	m=1	m=2	m=2
71.26	139.72	91.32	131.97	125.42	131.97	125.42	112.65	
120.03	233.14	104.20	177.72	117.37	177.72	117.37	130.25	
87.79	151.04	113.26	154.22	121.88	154.22	121.88	150.54	
104.51	189.23	108.65	151.00	127.81	151.00	127.81	131.75	
94.91	162.79	112.17	171.15	132.08	171.15	132.08	153.98	
99.22	174.80	109.94	147.03	133.11	147.03	133.11	135.01	
97.70	169.94	111.24	170.16	133.88	170.16	133.88	148.15	
97.83	170.60	110.54	152.38	133.61	152.38	133.61	140.08	
98.31	172.10	110.88	160.59	133.95	160.59	133.95	143.46	
97.68	169.96	110.74	159.22	133.66	159.22	133.66	143.13	
98.26	172.06	110.78	162.05	133.92	162.05	133.92	141.68	
97.81	170.33		155.18	133.69	155.18	133.69	143.86	
98.13	171.60		160.57	133.89	160.57	133.89	141.69	
97.91			157.27	133.72	157.27	133.72	143.45	
			152.28		152.28		142.24	
			152.72		152.72		142.92	
							142.66	
							142.63	

Table 4.2 : Effect of starting functions, initial eigen value and computations in double precision

λ_1	λ_2	λ_3	λ_4	λ_5
71.26	56.15	71.26	84.23	71.26
120.03	144.76	120.03	128.64	120.03
87.79	78.58	87.79	82.92	87.79
104.51	116.71	104.51	101.43	104.51
94.91	89.23	94.91	92.98	94.91
99.22	103.34	99.22	99.13	99.22
97.70	95.50	97.20	96.53	97.70
97.83	98.92	97.83	97.24	97.83
98.31	97.83	98.31	97.58	98.31
97.68	97.79	97.68		97.68
98.26		98.26		98.26
97.81		97.81		97.81
98.13		98.13		98.13
97.91		97.91		97.91

Table 4.3 : Convergence study of buckling load in various model schemes.

λ (Model 2)	λ (Model 3)	λ (Model 4)	λ (Model 5)	λ (Model 6)
263.31	1383.14	187.62	184.75	61.14
64.87	64.60	84.54	70.83	132.29
79.72	69.84	69.82	77.19	72.51
76.87	66.65	73.57	77.87	79.35
87.41	94.85	86.00	84.86	79.24
78.01	77.13	84.39	79.78	
82.65	79.39	79.67	81.52	
80.08	82.26	79.58	80.69	
81.86	80.53		81.42	
80.62	81.41		80.92	
81.39	80.88		81.19	
			81.04	
			81.14	
			81.07	

Table 4.4 : Effect of number of layers in model 5.

λ (2 layers)	λ (4 layers)	λ (6 layers)	λ (20 layers)	λ (50 layers)
410.77	1381.17	1382.85	1394.92	1399.87
96.69	69.62	66.21	60.81	60.47
78.98	64.12	67.93	81.24	82.10
75.32	58.96	63.52	82.30	85.67
74.46	69.96	96.43	88.14	86.01
74.25	74.90	76.73	83.63	
	78.67	83.08	86.53	
	74.62	78.99	84.91	
	74.74	82.46	85.80	
		81.74	85.27	

Table 4.5 : Effect of starting functions and length to thickness ratios in model 5

λ_{s_1}	λ_{s_2}	λ_{s_3}
184.75	1382.85	4045.26
70.89	66.21	64.19
77.20	67.93	66.18
77.87	63.52	59.07
84.86	96.43	90.28
79.78	76.73	75.57
81.52	83.08	85.18
80.69	78.99	78.06
81.42	82.46	82.74
80.92	80.46	80.23
81.19	80.86	81.66
81.04	81.24	80.76
81.14	81.02	81.31
81.07	81.14	80.97
	81.07	81.13
		81.07

Table 4.6 : Convergence study of constants of integration and displacement functions in model B.

Displacements Functions	$\eta =$										
	0.1	0.1	0.2	0.3	0.4	0.5	0.6	0.7	0.8	0.9	1.0
u_n	0	0.551	0.883	0.984	0.892	0.664	-0.401	0.171	0.042	0.007	0
u_{n+1}	0	-0.003	-0.041	-0.177	-0.404	-0.662	-0.893	-0.982	-0.885	-0.541	0
v_n	0	0.913	1.118	0.871	0.401	-0.072	-0.401	-0.543	-0.511	-0.331	0
v_{n+1}	0	-0.334	-0.523	-0.541	-0.392	-0.063	0.412	0.883	1.143	0.924	0
w_n	0	0.132	0.411	0.701	0.920	1.000	0.920	0.701	0.411	0.132	0
w_{n+1}	0	0.132	0.412	0.703	0.920	1.000	0.920	0.703	0.412	0.132	0

Eigen value	k_1	k_2	k_3	k_4
81.13	-1046.29	166.23	-22.43	-5.58
80.07	-1186.33	165.07	66.95	26.80

Table 4.7 : Convergence study of particular integral terms in model 5

Eigen Values	H ₁	H ₂	H ₃	H ₄	H ₅	H ₆	H ₇	H ₈	H ₉	H ₁₀	H ₁₁
79.34	11.09	-2.57	2.91	1.98	-4.02	-0.43	10.57	3.44	2.74	7.30	0.40
82.21	11.10	-2.57	2.90	1.98	-4.03	-0.42	10.57	3.44	2.77	7.29	0.41
81.36	11.14	-2.57	2.91	2.00	-4.05	-0.43	10.57	3.44	2.77	7.29	0.41
80.863	11.11	-2.57	2.91	1.99	-4.04	-0.43	10.57	3.44	2.77	7.29	0.41

Table 4.8 : Iterated eigen values in solution using
two variables v and w

λ_0 (Model 1)		λ_0 (Model 2)	
(m=1)	(m=2)	(m=1)	(m=2)
415.7	129.05	2147.	
61.65	130.03	57.34	
69.48	129.80	112.4	
176.60	129.86	56.40	
60.59		117.0	
891.80		56.19	
59.02			
190.90			
50.17			
193.40			
59.10			
192.90			
59.20			

CHAPTER V

CONCLUSIONS

The present work is a moderate contribution to the analysis of composite plates. Based on the results obtained certain conclusions can be drawn.

- 1a. Successive iteration technique works well in the buckling and free vibration problems of decoupled thin antisymmetric angle ply laminates. The technique gives slightly higher eigen values compared to other solution techniques.
- b. The computational efficiency is high and the solution converges closely with the results of other techniques. In many of the cases the solution is obtained in atmost five iterations.
- c. Programming requires less effort and for different boundary conditions the changes to be made are only in finding the values the constants of integration.
- d. A mesh size of 0.01 interval in quadrature using trapezoidal rule is sufficient. Convergence criteria of $(\lambda_{n+1} - \lambda_n) / \lambda_{n+1} \geq 0.01$ for the two successive iterations to converge is sufficient for accuracy.
- e. The technique converges to the same eigenvalue, even if different initial functions are used.

In thin composite plate buckling problems with SS, SC and CC boundary conditions, optimization can be made with respect to fibre orientation using this technique. To increase the load carrying capacity in CF, SF and FF condition, the laminate has to be designed for $\theta = 0$ fibre orientation. The buckling load increases as the aspect ratio increases. For various biaxial loading ratios interaction curves can be drawn with this technique, which will be useful in design.

- g. In free vibration problems with CC condition the plate has to be designed for $\theta = 90^\circ$ and in FF condition for $\theta = 0^\circ$ to increase the natural frequency. As the aspect ratio increases, the natural frequency decreases, reaches minimum and then increases in CC and SS condition whereas it drops continuously in FF condition.
- h. The technique can be applied readily, in optimal design of laminates, as it consumes less computational time. In optimization process the analysis has to be repeated many times for various parameters.
- i. Optimization studies can be made in hybrid thin anti-symmetric angle ply laminates, as it is possible to analyse decoupled thin laminates, using this technique.
- j. The present study has been made, using small deformation theory. Optimization studies may be performed in large deformation domain.

Fibre volume fractions in addition to fibre orientations of laminae can be taken in optimal design.

2. Successive iteration technique, when attempted in thin coupled antisymmetric laminate buckling problem failed to give correct eigen value λ , even though positive convergence in λ is achieved. Various model schemes have been tried to investigate the failure of the method. The method seems to be doubtful when the number of dependent variables more than one appear in the governing equations. The solution process may be sensitive to the values of the coefficients of the derivatives appearing in the governing equations. The present study is unable to pinpoint the reasons behind the failure of the method.

REFERENCES

1. Timoshenko, S.P. and Krieger, S.W., Theory of plates and shells, 2nd edn., McGraw Hill, New York, 1959.
2. Harris, G.Z. The buckling of orthotropic rectangular plates including the effect of lateral edge restraint, Int. J. Solids Struct. 11(7/8), 877-885.
3. Warren, F. and Norris, C.B., Mechanical properties of a laminate designed to be Isotropic, Rept. 1841, May, 1953, Forest products Lab., Madison, Wisconsin.
4. Bartholmew, P., Ply stacking sequence for laminated plates having inplane and bending orthotropy, Royal Aircraft Establishment, TR-76003, 1976.
5. Ambartsumyan, S.A., Theory of anisotropic shells, TTF-11B, May 1964, NASA.
6. Holston, A., Jr., Buckling of orthotropic plate with one free edge, AIAA Journal, Vol. 3, 7, 1970, 1352-1354.
7. Sharma, Iyengar and Murthy, A study of coupling in laminated plates, Fibre science and technology, 18 (1983), 287-299.
8. Jones, Robert M, Harold S. Morgan and James M. Whitney, Buckling and vibration of antisymmetrically laminated angle-ply rectangular plates, J. Appl. Mech., December, 1973, pp. 1143-1144.
9. Housner, J.M. and Stein, M. Numerical analysis and parametric studies of the buckling of composite orthotropic compression and shear panels, Technical note NASA TN D-7996, Oct. 1975.
10. Paul, A, Logace, David W. Jensen and Douglas C. Finch, Buckling of unsymmetric composite laminate, An International journal on composite structures, Vol. 5, No. 2, 1986.
11. Klaus Rohwer, Bending-twisting coupling effects on the buckling load of symmetrically stacked plates, DFVLR, Institute for Strukturmechanik Brannschurig, Germany.
12. Whitney, J.M. and Leissa, A.W., Analysis of Heterogeneous anisotropic plates, J. Appl. Mech. 36(2), 1969, 261-266.

13. Jones, R.M., Mechanics of composite materials, Scripta, Washington, D.C., 1975.
14. Wittrick, W.H., Rationalisation of anisotropic buckling problems, contribution to the theory of aircraft structure Van der Neut anniversary volume, Delft Univ. Press, Delft, Netherlands, 359-377.
15. Reissner, E. and Stavasky, Y, Bending and stretching of certain type of heterogeneous anisotropic elastic plates, J. Appl. Mech., 9, 1961, 402-408.
16. Ashton, J.E., Approximate solutions for unsymmetrical laminated plates, J. Composite Mat. 3, 1969, 189-191.
17. Barwey, D., Optimal design of laminated composite plates, M. Tech. thesis, Dept. of Aero. Engg., Indian Institute of Technology, Kanpur, 1985.
18. Sharma, S., Iyengar, N.G.R. and Murthy, P.N., Buckling of antisymmetric cross and angle-ply laminated plates, Int. J. Mech. Sc. 22, 607-20, 1980.
19. Whitney, J.M., The effect of boundary condition on the response of laminated composites, J. Comp. materials 4 (1970), 192-203.
20. Bert, C.W. and Mayberry, B.L., Free vibration of unsymmetrically laminated anisotropic plates with clamped edges, J. Comp. Material, Vol. 3 (1969), pp. 282-293.
21. Lin, C.C. and King, W.W., Free transverse vibrations of rectangular unsymmetrically laminated plates, 36(1), (1974), pp. 91-103.
22. Kamal, K. and Durvasula, S., Some studies on free vibration of composite laminates, Composite structures 5 (1986), pp. 177-202.
23. , Optimal design of hybrid composite laminated plates under inplane loading, M.Tech. thesis, Dept. of Aero Engg., Indian Institute of Technology, Kanpur, 1987.
24. J.N. Reddy and C.W. Chao, A comparison of closed form and finite element solutions of thick laminated anisotropic rectangular plates. Nucl. Engng. Des. 64, 153-167 (1981).
25. J.N. Reddy, A sample higher order theory for laminated plates, J. Appl. Mech., 51, 745-752 (1984).